# Thermoelectric Figure of Merit of Two-Dimensional Materials in a Magnetic Field

by

Al-Thaddeus Avestruz

Submitted to the Department of Physics
in partial fulfillment of the requirements for the degree of

Bachelor of Science in Physics

at the

MASSACHUSETTS INSTITUTE OF TECHNOLOGY

May 1994



Author .....
Department of Physics
May 18, 1994

Certified by .....
Mildred Dresselhaus
Institute Professor
Thesis Supervisor

Accepted by .....
Professor Aaron Bernstein
Chairman, Departmental Committee on Undergraduate Students

# Thermoelectric Figure of Merit of Two-Dimensional Materials in a Magnetic Field

by

Al-Thaddeus Avestruz

Submitted to the Department of Physics
on May 18, 1994, in partial fulfillment of the
requirements for the degree of
Bachelor of Science in Physics

## Abstract

A theoretical treatment on the effect of a magnetic field on the thermoelectric figure of merit ZT for two-dimensional (2D) materials is presented. The figure of merit is a function of three transport coefficients: the electrical conductivity, the Seebeck coefficient or thermopower, and the total thermal conductivity. The total thermal conductivity consists of contribution from electrons and phonons to energy transport. For any magnetic field, in two- or three-dimensions, the limiting factor in ZT is the phonon contribution to the thermal conductivity. The phonon thermal conductivity is an intrinsic property which cannot be changed without significantly changing the other properties of the material. The other coefficients can be optimized relative to each other by varying the chemical potential by doping and by the application of a magnetic field.

The figure of merit was investigated at various ranges of magnetic field. The ranges of a magnetic field can be categorized into three regions: the low-field or semiclassical case, the quantum or Landau-level case, and the high-field case. The low-field case is treated in the context of the relaxation time approximation of the semiclassical Boltzmann equation. The Landau-level case is treated first by the ad hoc extension of the semiclassical equations by using magnetically-quantized density of states; secondly, by the Born approximation for Landau-level broadening. The high-field case is qualified by the ground state Landau-level being much greater than the Fermi energy; this case can be treated semiclassically. Various approximations are used for the various cases to provide analytical results and to simplify numerical calculation.

Under conditions of Landau-level quantization, an effect referred to as carrier dumping occurs. This results in carrier pockets with low cyclotron effective masses emptying into pockets with high cyclotron effect mass. This effect is due to the pinning of the Fermi energy to the nearest Landau-level. This can result significant increases in ZT by dumping all the carriers into a pocket with the most favorable orientation.

Two thermoelectric materials, bismuth and bismuth telluride, are used as test

cases for the application of the theory presented. The quantitatively favorable with respect to the current state of experimental knowledge.

Thesis Supervisor: Mildred Dresselhaus
Title: Institute Professor

# Acknowledgments

I'd like to thank Mom and Dad for their support in my education, my brother Mark for his help, and my sister Camille. I am deeply grateful to Professor Dresselhaus for supporting my work and supervising this thesis. I'd also like to thank Lyndon Hicks for his help in the research and guiding of this thesis.

# Contents

# List of Figures

# Chapter 1

# Introduction

Thomas Seebeck, in 1821, discovered that a potential difference could be induced by heating a junction of two dissimilar metals. This thermoelectric effect is related to another phenomenon later discovered by Jean Peltier in 1834. He found that a current passing through a junction of dissimilar materials caused a cooling of one end and a heating of the other.[3, p.1] This cooling effect held promise for a method of electronic refrigeration.

The first theoretical attempt at relating these two effects was made in 1855 by Lord Kelvin using thermodynamic arguments.[4, p.1] He reconciled what are now known as the Seebeck effect and the Peltier effect. He also predicted what is now known as the Thomson effect in which a current dependent cooling and heating effect occurs through a uniform conductor.

The thermoelectric properties are enhanced by the application of a magnetic field. A discovery known as the Ettinghausen effect which results in a transverse heat flow from a longitudinal current in homogeneous conductor in a magnetic field. This led to measurements which confirmed magneto-thermoelectric and thermomagnetic effects.[3, p. 2]

In 1993, Hicks et al. predicted that a significant enhancement of thermoelectric properties of a material occurs as its dimensionality is lowered.[6] They have predicted that the thermoelectric figure of merit[1] of a material which behaves as

[1]The thermoelectric figure of merit (Z) is a quantification of the useful properties for the various

a two-dimensional conductor has at least a three-fold higher figure of merit than one that behaves three-dimensionally. In a follow-up paper, they calculated an even higher figure of merit for a one-dimensional conductor.[2][7] In this calculation, they predict at least an order of magnitude higher figure of merit for very thin ($< 10\mathring{A}$) one-dimensional wires.

The figure of merit calculation using semiclassical theory for 3D bulk materials is in good agreement with experiment, compared both by Hicks and others. It has been also shown experimentally that the figure of merit in 3D bulk materials is increased in a magnetic field. Harman et al. carried out a detailed calculation for the transport coefficients of bulk bismuth in a magnetic field using tensors to represent the anisotropies and the tilts of each of the carrier pockets[13]. He then compared the numerical results of his calculations with experiment and found them in agreement[14].

It seems that lower dimensionality in materials causes a significant increase in the figure of merit; although, this has not yet been verified experimentally. An applied magnetic field is also known to effect moderate gains in figure of merit, although not quite as dramatic as the gains from the dimensionality effect.

In high magnetic fields, where quantum effects are manifested in Landau-levels, a confinement similar to a decrease in dimensionality is possible and a strong effect on figure of merit is predicted. In this regime, an effect in materials with tilted multiple-carrier pockets results in what is known as *carrier-pocket dumping* when the Landau-level spacings become large enough. This effect can be used to cause transport to occur in the single most favorable pocket.

In this thesis, I calculate the effect of a magnetic field on the thermoelectric properties of low-dimensional materials. In addition, some predictions will be made for $Bi$ and $Bi_2Te_3$, two thermomelectric materials, in a magnetic field, which as a thin film behave two-dimensionally. In these discussions, much of the algebra is omitted, but some key calculations are included in the appendices.

---

thermoelectric effects.

[2]They show that part of this increase is due to a decrease in lattice thermal conductivity due to a reduction of phonon propagation modes.

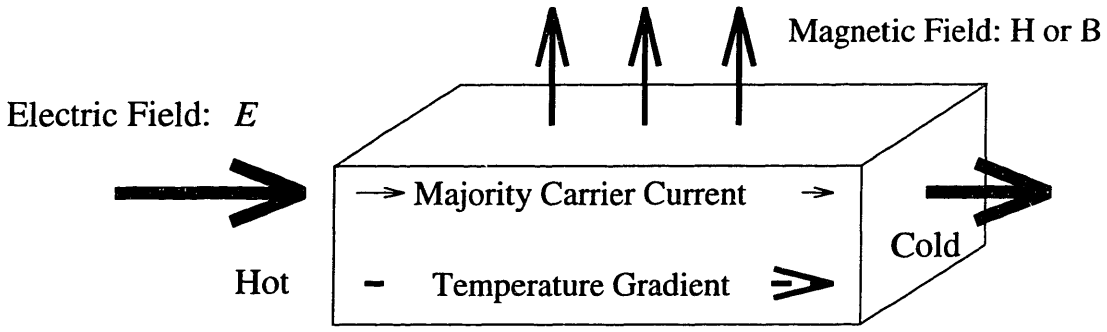


Figure 1-1: The general configuration for the longitudinal magneto-Seebeck effect is shown above. This is the configuration from which the magneto-transport coefficients for the Seebeck effect are later calculated.

# Chapter 2

# Background

## 2.1 Thermoelectric Figure of Merit

The thermoelectric figure of merit Z is used to determine whether a material is a good thermoelectric cooler. The figure of merit Z is defined as [4]:

$$Z \equiv \frac{\alpha^2 \sigma}{\kappa} \tag{2.1}$$

where $\alpha$ is the Seebeck coefficient, $\sigma$ is the electrical conductivity and $\kappa$ is the total thermal conductivity.

$$\kappa = \kappa_e + \kappa_{ph}, \tag{2.2}$$

the electronic and thermal contribution to the thermal conductivity.

The transport coefficients $\sigma$, $\alpha$ and $\kappa$, for isotropic materials are defined as,

$$\sigma = \frac{\mathcal{E}_x}{i_x}; \quad \{i_y = i_z = 0, \ \nabla T = 0\}, \tag{2.3}$$

$$\alpha = \frac{\mathcal{E}_x}{\partial T/\partial x}; \quad \{\mathbf{i} = 0, \ \frac{\partial T}{\partial y} = \frac{\partial T}{\partial z} = 0, \}, \tag{2.4}$$

$$\kappa = \frac{-w_x}{\partial T/\partial x}; \quad \{\mathbf{i} = 0, \ \frac{\partial T}{\partial y} = \frac{\partial T}{\partial z} = 0\}, \tag{2.5}$$

where $\mathbf{i}$ is the electric current density, $\mathbf{w}$ is heat flow rate density and $T$ is the

temperature.

## 2.2 Boltzmann Equation

The basis for the semiclassical calculation of the transport coefficients is based on the steady-state solution to the Boltzmann equation.[1] The generalized Boltzmann equation is based on an averaged carrier density approximation and is given by [11, p.189],

$$\frac{df}{dt} = \frac{\partial f}{\partial t} + \dot{\mathbf{k}} \cdot \nabla_{\mathbf{k}} f + \dot{\mathbf{r}} \cdot \nabla_{\mathbf{r}} f = \left.\frac{\partial f}{\partial t}\right|_{collision} \tag{2.6}$$

The Boltzmann equation gives us the behavior of the carrier density in $\mathbf{r}$ and $\mathbf{k}$-space in the presence of an external force. These forces may be due to an electric field, magnetic field, or a temperature gradient.

In the steady state,

$$\frac{\partial f}{\partial t} = 0$$

Hence,

$$\dot{\mathbf{k}} \cdot \nabla_{\mathbf{k}} f + \dot{\mathbf{r}} \cdot \nabla_{\mathbf{r}} f = \left.\frac{df}{dt}\right|_{collision}, \tag{2.7}$$

where,

$$\dot{\mathbf{k}} = -\frac{e}{\hbar}(\vec{E} + \vec{v} \times \vec{B}), \tag{2.8}$$

which is the quantum mechanical analog of the classical Lorentz force;

$$\dot{\mathbf{r}} = \frac{1}{\hbar} \nabla_{\mathbf{k}} E(\mathbf{k}), \tag{2.9}$$

which is the group velocity of the carrier wave packet. [11, p.190]

This steady-state equation is an accounting of the possible processes in $\mathbf{k}$ and $\mathbf{r}$-space under time-invariant conditions. It conserves $\mathbf{k}$-space volume for the combined scattering, diffusion and external force processes in equilibrium.

[1] Appendix A gives a derivation.

If we assume a simplifying form known as the relaxation time approximation,

$$\frac{df}{dt} = -\frac{f - f_0}{\tau}, \tag{2.10}$$

then the solution is in closed form,

$$f = f_0 + C \exp\left(-\frac{t}{\tau}\right). \tag{2.11}$$

Equation 2.11 shows that when the external force is removed, the carrier distribution decays exponentially with a time constant $\tau$ to equilibrium steady-state distribution $f_0$. There are limitations to this approximation; it is necessary to assume that there are only small deviations from $f_0$, and that $\tau$ and $f_0$ are independent of the external forces.

## 2.3 Electron and Heat Currents

A generalized calculation from the thermodynamics of irreversible processes yields relations without the restrictions of the Boltzmann equation calculations [11, p.200]. An important contribution by Smrčka and Středa [12] is the generalization of the Kubo formulae for elastic scattering in the context of single electron theory. The approach they chose replaced the thermal gradient by a gravitational potential in order to take advantage of a perturbational form of the Hamiltonian. The general form used for the electron and heat currents are

$$\vec{\mathbf{J}_e} = L_{11}\left[\vec{E} - \frac{T}{e}\nabla\left(\frac{\zeta}{T}\right)\right] + L_{12}\left[T\nabla\left(\frac{1}{T}\right) - \nabla\psi\right] \tag{2.12}$$

$$\vec{\mathbf{J}_q} = L_{21}\left[\vec{E} - \frac{T}{e}\nabla\left(\frac{\zeta}{T}\right)\right] + L_{22}\left[T\nabla\left(\frac{1}{T}\right) - \nabla\psi\right], \tag{2.13}$$

where $\vec{E} = -\nabla\phi$, and $\phi = \vec{r}\cdot\vec{E}$ and $\psi = \vec{r}\cdot\nabla\psi$ are the electric and thermal potentials, respectively.

The transport coefficients in terms of the elements of tensor $\overleftrightarrow{\mathbf{L}}$ are

$$\overleftrightarrow{\sigma} = \mathbf{L}_{11} \tag{2.14}$$

$$\overleftrightarrow{\alpha} = T^{-1}(\mathbf{L}_{11}^{-1}\mathbf{L}_{12} - \zeta/e) \tag{2.15}$$

$$\overleftrightarrow{\kappa} = T^{-1}(\mathbf{L}_{22} - \mathbf{L}_{21}\mathbf{L}_{11}^{-1}\mathbf{L}_{12}) \tag{2.16}$$

These equations obey the Onsager relations for an arbitrary tensor $\overleftrightarrow{R}$ which are given by,

$$R_{ik}(\vec{U}) = \overline{R_{ki}}(-\vec{U}). \tag{2.17}$$

These Onsager relations are important in considering whether a theory yields physical results. For example, in the conductivity tensor $\sigma_{xy} = -\sigma_{yx}$. This is also true for the thermopower, $\alpha_{xy} = -\alpha_{yx}$. However, one finds that with two dimensional density of states that the thermopower violates these Onsager relations if the contributions of microscopic surface currents due to magnetization are not taken into account.[12, p.2156–2157]

## 2.4 Boltzmann Equation for Anisotropic Materials

In my discussions of the semiclassical calculations, I will follow the approach of Harman and Honig [5, pp. 241-257] of a multi-valley model based on the semiclassical Boltzmann equation. Their discussion is based on a generalized multi-valley model with elliptical-band dispersion relations.

The calculations are based on the relaxation time approximation to the semiclassical Boltzmann equation,

$$\frac{\partial f}{\partial t} = -\frac{f - f_0}{\tau} = \frac{\boldsymbol{\Psi} \cdot \vec{v}}{\tau} \frac{\partial f}{\partial \mathcal{E}}. \tag{2.18}$$

In generalizing $\tau$ for anisotropic materials, the anisotropic relaxation time is rep-

resented as a tensor.

$$\frac{\partial f}{\partial t} = (\overleftrightarrow{\nu} \cdot \mathbf{\Psi}) \cdot \vec{v}\, \frac{\partial f_0}{\partial \mathcal{E}}, \tag{2.19}$$

where f is the distribution function, $f_0$ is the Fermi-Dirac distribution [9, p. 80] given by

$$f_0 = \frac{1}{e^{(\mathcal{E}-\zeta)/k_B T} + 1}, \tag{2.20}$$

$\vec{v}$ is the carrier group velocity vector, $\overleftrightarrow{\nu}$ is the reciprocal of the relaxation time tensor $\overleftrightarrow{\tau}$, $\zeta$ is the chemical potential and

$$\mathbf{\Psi} \equiv \overleftrightarrow{\tau} \cdot \mathbf{\Psi}^* = \frac{\overleftrightarrow{\tau} \cdot \{\mathbf{F} + e^2(\mathbf{F} \cdot \mathbf{H})(\mathbf{C} \cdot \mathbf{H}) + Ze[(\overleftrightarrow{\tau} \cdot \mathbf{F}) \cdot \overleftrightarrow{\mathbf{q}}] \times \mathbf{H}\}}{1 + e^2[\mathbf{H} \cdot (\mathbf{C} \cdot \mathbf{H})]}. \tag{2.21}$$

$\overleftrightarrow{\mathbf{q}}$ is the reciprocal of the effective mass tensor $\overleftrightarrow{\mathbf{m}}$, $\mathbf{H}$ is the applied magnetic field, and

$$\mathbf{C} = \frac{\overleftrightarrow{\mathbf{m}} \cdot \overleftrightarrow{\nu}}{|\overleftrightarrow{\mathbf{m}}|\, |\overleftrightarrow{\nu}|}. \tag{2.22}$$

In Equation 2.21, $\mathbf{F}$, is the force external to the system,

$$\mathbf{F} \equiv +Ze\,\nabla_{\mathbf{r}}\,\frac{\epsilon_B}{e} - T\nabla_{\mathbf{r}}\,\frac{\mu}{T} - \frac{\mathcal{E}}{\mathcal{T}}\nabla_{\mathbf{r}}\,T, \tag{2.23}$$

where $Z$ is the charge of the carrier $\{+1$ for electrons, -1 for holes$\}$ and $\epsilon_B$ is the band-edge.

Equation 2.21 is the generalized impulse due to effective external force on the carriers in the anisotropic material. This equation can be simplified for a single ellipsoidal pocket by choosing orthogonal directions of field which coincide with the principal axes of the crystal. In the same way, the effective mass tensor can be made diagonal along the principal axes of the first Brillouin zone.

## 2.5 Magnetic Field

An alternate calculation for the effect of the magnetic field which is not restricted by the requirements of a cyclotron radius larger than the deBroglie wavelength of

the wavepocket and $\omega_c\tau \ll 1$ is performed by Ziman [15]. An alternate coordinate system is used which uses the phase relationships of orbiting electrons to carry out a Boltzmann calculation.

As in Equation 2.8, the change of the wavevector is given by

$$\dot{\mathbf{k}}_B = \frac{e}{\hbar}(\vec{v} \times \vec{B}) \tag{2.24}$$

Changes in the wavevector are mutually orthogonal to the magnetic field and to $\vec{v}$. The magnetic field forces the electron into an orbital plane in which the energy is conserved. The period of this orbit is given by,

$$T = \frac{2\pi}{\omega_c} = \frac{\hbar}{eB}\oint \frac{dk}{v_\perp} \tag{2.25}$$

The cyclotron frequency is then calculated as

$$\omega_c = \frac{eB}{m_c^*} \tag{2.26}$$

and the orthogonal component of the group velocity is given by

$$v_\perp = \frac{1}{\hbar}\frac{d\epsilon}{k_\perp} \tag{2.27}$$

where $k_\perp$ is the orthogonal component of the wavevector.

In choosing new $k$-space coordinates, $\epsilon(\mathbf{k})$ is constant. The angular component of the coordinate is given by

$$\theta = \omega_c \frac{\hbar}{eB}\oint_{\mathbf{k}} \frac{dk}{v_\perp}. \tag{2.28}$$

and the cyclotron effective mass is

$$\begin{aligned} m_c^* &= \frac{\hbar}{2\pi}\oint \frac{dk}{v_\perp} \\ &= \frac{\hbar^2}{2\pi}\frac{d\mathcal{A}}{d\epsilon}; \end{aligned} \tag{2.29}$$

$\mathcal{A}$ is the area circumscribed by the orbit.

In the steady-state Boltzmann equation, the magnetic interaction term is then,

$$\left.\frac{\partial f}{\partial t}\right]_{mag} = \theta\frac{\partial g}{\partial \theta} = \omega_c\frac{\partial g}{\partial \theta}. \tag{2.30}$$

Substituting this into Equation 2.6 in the context of the relaxation time approximation,

$$e\vec{E}\cdot\vec{v}\left(-\frac{\partial f_0}{\partial \epsilon}\right) = \frac{g}{\tau} + \omega_c\frac{\partial g}{\partial \theta}. \tag{2.31}$$

The solution of this differential equation is given by [15, p.301]

$$g = -\frac{e}{\omega_c}\frac{\partial f_0}{\partial \epsilon}\int_{-\infty}^{\theta}\mathbf{v}\exp\left[\frac{(\theta'-\theta)}{\omega_c\tau}\right]d\theta\cdot\vec{E}. \tag{2.32}$$

The electron current is then

$$\vec{\mathbf{J}}_e = 2\int e\,\mathbf{v}_\mathbf{k}\,g_\mathbf{k}\,d\mathbf{k} \tag{2.33}$$

and the heat current is

$$\vec{\mathbf{J}}_q = 2\int e\,\mathbf{v}_\mathbf{k}\,g_\mathbf{k}\,d\mathbf{k}. \tag{2.34}$$

## 2.6 Two-Dimensional System

A free particle which can move along a plane, but is bound in the direction orthogonal to that plane is said to behave two-dimensionally. This occurs in real materials when the thickness of a thin film is of the order of the deBroglie wavelength of the electron in the material. For example, a thin film in the $x$-$y$ plane is bound in the $\hat{z}$-direction; thhe behavior of the electron along this axis cannot be described classically, but rather, by bound states.

The behavior of the electron in the $\hat{x}$, $\hat{y}$-directions are described by plane waves. The solution to the the two-dimensional time-independent Hamiltonian

$$(\frac{\hbar^2}{2m}\nabla^2 + \mathcal{V})\psi = E_n\psi, \tag{2.35}$$

is given by these plane wave solutions and a bound state solution.

$$\psi = \phi_x e^{ik_x x} \phi_y e^{ik_y y} \phi_z \sin k_z z \tag{2.36}$$

This solution leads to the dispersion relation given by,

$$\varepsilon(k_x, k_y) = \frac{\hbar^2}{2}\left(\frac{k_x^2}{m_x} + \frac{k_y^2}{m_y} + \frac{\pi^2}{m_z a^2}\right) \tag{2.37}$$

## 2.7 Hicks Calculations

Lyndon Hicks et al. show the improvements in the thermoelectric figure of merit Z over the 3D bulk value. [6] The focus of their paper is the use of $Bi_2Te_3$ superlattices as thermoelectric refrigeration elements. They also show that the high anisotropy of certain materials like $Bi_2Te_3$ can be taken advantage of, to increase Z. In their calculations, they assume anisotropic, but diagonal effective masses $(m_x, m_y, m_z)$ and mobilities $(\mu_x, \mu_y, \mu_z)$, and isotropic relaxation time, $\tau$.

### 2.7.1 Z of a 3D bulk material

Assuming an ellipsoidal dispersion relation given by

$$\varepsilon(k_x, k_y, k_z) = \frac{\hbar^2}{2}\left(\frac{k_x^2}{m_x} + \frac{k_y^2}{m_y} + \frac{k_z^2}{m_z}\right), \tag{2.38}$$

the following transport coefficients for carrier current, temperature gradient, and electric field in the $\hat{x}$-direction were calculated:

$$\sigma = \frac{1}{2\pi}\left(\frac{2k_B T}{\hbar^2}\right)^{3/2} (m_x m_y m_z)^{1/2} F_{1/2} e\mu_x, \tag{2.39}$$

$$\alpha = -\frac{k_B}{e}\left(\frac{5F_{3/2}}{3F_{1/2}} - \eta^*\right), \tag{2.40}$$

$$\kappa_e = \frac{\tau\hbar^2}{6\pi^2}\left(\frac{2k_B T}{\hbar^2}\right)^{5/2}\left(\frac{m_y m_z}{m_x}\right)^{1/2} \times k_B\left(\frac{7}{2}F_{5/2} - \frac{25F_{3/2}^2}{6F_{1/2}}\right), \tag{2.41}$$

where $F_j$ is the Fermi-Dirac distribution function

$$F_j = F_j(\eta^*) = \int_0^\infty \frac{\xi^j}{\exp(\xi - \eta^*) + 1} d\xi, \tag{2.42}$$

$\eta^* = \zeta / k_B T$ is the reduced chemical potential relative to the conduction band edge.

They find that $Z_{3D}$, including the phonon contribution to thermal conductivity $\kappa_{ph}$,

$$Z = \frac{\alpha^2 \sigma}{\kappa_e + \kappa_{ph}}, \tag{2.43}$$

is given by

$$Z_{3D}T = \frac{\frac{3}{2}\left(\frac{5F_{3/2}}{3F_{1/2}} - \eta^*\right)^2 F_{1/2}}{\frac{1}{B} + \frac{7}{2}F_{5/2} - \frac{25F_{3/2}^2}{6F_{1/2}}}, \tag{2.44}$$

where

$$B = \frac{1}{3\pi^2}\left(\frac{2k_B T}{\hbar^2}\right)^{3/2} (m_x m_y m_z)^{1/2} \frac{k_B^2 T \mu_x}{e\kappa_{ph}}. \tag{2.45}$$

Two parameters which could be varied are the reduced chemical potential $\eta$ and B. $\eta$ can be varied by changing the carrier concentration by doping. B is a parameter which depends on the intrinsic properties of the material.

### 2.7.2 Z of a 2D Quantum Well

In their calculation for the Z of a quantum well, Hicks et al. made several assumptions. They assumed that the ground state band of the quantum well is the only one occupied and that there is no inter-band scattering. In addition, if this single well were part of a superlattice, there would be no inter-well scattering or tunneling. The semiconductor is assumed to be a wide-gap semiconductor with no intervalley scattering. The layers are in the $\hat{x}$-$\hat{y}$ plane and a current in the $\hat{x}$-direction.

An elliptical dispersion relation for an anisotropic material is used,

$$\varepsilon(k_x, k_y) = \frac{\hbar^2}{2}\left(\frac{k_x^2}{m_x} + \frac{k_y^2}{m_y} + \frac{\pi^2}{m_z a^2}\right). \tag{2.46}$$

Deriving the transport coefficients in a similar manner to § 2.7.1, from the Boltzmann

equation,

$$\sigma = \frac{1}{2\pi a}\left(\frac{2k_BT}{\hbar^2}\right)(m_xm_y)^{1/2}F_0e\mu_x, \tag{2.47}$$

$$\alpha = -\frac{k_B}{e}\left(\frac{2F_1}{F_0} - \eta^*\right), \tag{2.48}$$

$$\kappa_e = \frac{\tau\hbar^2}{4\pi a}\left(\frac{2k_BT}{\hbar^2}\right)^2\left(\frac{m_x}{m_y}\right)^{1/2}k_B\left(F_2 - \frac{4F_1^2}{F_0}\right), \tag{2.49}$$

where $a$ is the thickness of the layer, or equivalently, the thickness of the well,

$$\eta^* = \frac{1}{k_BT}\left(\eta - \frac{\hbar^2\pi^2}{2m_za^2}\right). \tag{2.50}$$

Combining the coefficients, ZT is

$$Z_{2d}T = \frac{\left(\frac{2F_1}{F_0} - \eta^*\right)^2F_0}{\frac{1}{B'} + 3F_2 - \frac{4F_1^2}{F_0}}, \tag{2.51}$$

$$B' = \frac{1}{2\pi a}\left(\frac{2k_BT}{\hbar^2}\right)(m_xm_y)^{1/2}\frac{k_B^2T\mu_x}{e\kappa_{ph}}. \tag{2.52}$$

# Chapter 3

# Calculation of 3D Transport Coefficients

## 3.1 Semiclassical Calculation of the Magneto-transport Equations

The Hicks calculation can be extended using the methods of Harman and Honig to include the application of a magnetic field. This extension of formal Boltzmann theory to semiclassical statistics is only applicable for cases where the magnetic field is weak enough so that quantum effects are negligible. In general, this implies $\omega_c \tau \lesssim 1$.

### 3.1.1 Transport coefficients for 3D bulk material in a uniform magnetic field in the $\hat{z}$-direction

The transport coefficients $\alpha$, $\sigma$, $\kappa$ and Z are calculated assuming an ellipsoidal dispersion relation given by:

$$\varepsilon(k_x, k_y, k_z) = \frac{\hbar^2 k_x^2}{2m_x} + \frac{\hbar^2 k_y^2}{2m_y} + \frac{\hbar^2 k_z^2}{2m_z}. \tag{3.1}$$

The transport coefficients are given in terms of the following integrals:

$$\mathcal{S}_i = \int_0^\infty \frac{\xi^{r+i+1}}{1+\beta^2\xi^{2r-1}} \frac{\partial f_0}{\partial \xi} d\xi \tag{3.2}$$

$$\mathcal{H}_{q,i} = \int_0^\infty \mu_q \frac{\xi^{2r+i+1/2} B_z}{1+\beta^2\xi^{2r-1}} \frac{\partial f_0}{\partial \xi} d\xi, \tag{3.3}$$

where $B_z$ is the magnetic field in the z-direction, $\mu_q$ is the electron mobility in the $q^{th}$ direction, and r is the scattering parameter[1]. The reduced Fermi function is given by:

$$f_0 = \frac{1}{\exp(\xi - \eta) + 1} \tag{3.4}$$

where $\xi = \varepsilon / k_B T$, the reduced energy , and $\eta = \zeta / k_B T$, the reduced chemical potential, both relative to the edge of the conduction band. $\beta$ is the reduced magnetic field:

$$\beta^2 = \frac{e^2 \tau_0^2 B_z^2}{m_x m_y} = \mu_x \mu_y \Lambda^2 {B_z}^2. \tag{3.5}$$

The relaxation time coefficient is given as[5, p. ]:

$$\Lambda = \frac{3\mathcal{F}_{1/2}(\eta_e)}{2(r+1)\mathcal{F}_r(\eta_B)}, \tag{3.6}$$

where $\mathcal{F}_j$ is the Fermi-Dirac integral given below and $\eta_e$ and $\eta_B$ are the reduced Fermi energy of the carrier and the reduced band-edge energy, respectively..

The following transport coefficients were calculated:

$$\sigma = K \frac{{\mathcal{S}_0}^2 + \mathcal{H}_{x,0}\mathcal{H}_{y,0}}{\mathcal{S}_0} \tag{3.7}$$

$$\alpha = -\frac{k_B}{e}\left(\frac{\mathcal{S}_0\mathcal{S}_1 + \mathcal{H}_{x,0}\mathcal{H}_{y,1}}{{\mathcal{S}_0}^2 + \mathcal{H}_{x,0}\mathcal{H}_{y,0}} - \eta\right) \tag{3.8}$$

$$\kappa = K_1\left(\mathcal{S}_2 + \frac{\mathcal{S}_0\mathcal{H}_{x,1}\mathcal{H}_{y,1} - 2\mathcal{H}_{x,0}\mathcal{H}_{y,1}\mathcal{S}_1 - \mathcal{S}_0{\mathcal{S}_0}^2}{{\mathcal{S}_0}^2 + \mathcal{H}_{x,0}\mathcal{H}_{y,0}}\right), \tag{3.9}$$

[1] ...

where

$$K = \frac{16\, N_v\, \pi\, e\, \mu_x \sqrt{2}\sqrt{m_x}\sqrt{m_y}\sqrt{m_z}}{3\, h^3} (k_B T)^{3/2} \Lambda \tag{3.10}$$

$$K_1 = \frac{16\, N_v\, \pi\, \mu_x \sqrt{2}\sqrt{m_x}\sqrt{m_y}\sqrt{m_z}}{3\, h^3} (k_B T)^{5/2} \Lambda \frac{k_B}{e}, \tag{3.11}$$

where $N_v$ is the valley degeneracy and $m_x$, $m_y$, and $m_z$ are the principal effective masses for electrons.

Explicit analytical expressions are derivable only within certain approximations in terms of series. These simplifying approximations are plausible and useful for the ranges in which the semiclassical Boltzmann formalism is valid.

### 3.1.2 Small-field approximation, $\beta^2 \ll 1$

The transport integrals $\mathcal{S}_i$ and $\mathcal{H}_{q,i}$ cannot be approximated using a Taylor series over the integration bounds of zero to infinity due to the existence of complex poles over this region of convergence. However, the integrals may be piecewise approximated by two series:

$$\mathcal{S}_i = \int_0^{k/2} \left( \frac{\xi^{r+i+1}}{1+\beta^2 \xi^{2r-1}} \right) \frac{\partial f_0}{\partial \xi} d\xi + \int_{2k}^{\infty} \left( \frac{\xi^{r+i+1}}{1+\beta^2 \xi^{2r-1}} \right) \frac{\partial f_0}{\partial \xi} d\xi + \delta_S(k) \tag{3.12}$$

$$\mathcal{H}_{q,i} = \int_0^{k/2} \mu_q B_z \left( \frac{\xi^{2r+i+1/2}}{1+\beta^2 \xi^{2r-1}} \right) \frac{\partial f_0}{\partial \xi} d\xi + \int_{2k}^{\infty} \mu_q B_z \left( \frac{\xi^{2r+i+1/2}}{1+\beta^2 \xi^{2r-1}} \right) \frac{\partial f_0}{\partial \xi} d\xi + \delta_H(k) \tag{3.13}$$

where the radius of the poles in the complex plane is given by,

$$k = \left( \frac{1}{\mu_x \mu_y \Lambda^2 B_z^2} \right)^{\frac{1}{2r-1}} \tag{3.14}$$

and $\delta_K$ and $\delta_H$ are the error regions about the poles. These errors are exponentially small when the reduced Fermi energy $\eta$ is not near $k$. In cases where $\eta \approx k$, direct numerical integration over the error regions are necessary, or an appropriate analytic continuation is required for the approximation of the contributions to the transport coefficients about these poles. In this work, I have opted to perform direct numerical

integrations for the cases where $\eta \approx k$.

The series are approximated in terms of upper and lower Fermi-Dirac integrals:

$$F_j^+(\eta, b) \equiv \int_b^\infty \xi^j f_0(\eta) d\xi \tag{3.15}$$

$$F_j^-(\eta, b) \equiv \int_0^b \xi^j f_0(\eta) d\xi \tag{3.16}$$

which are related to the full Fermi-Dirac integrals:

$$F_j(\eta) \equiv \int_0^\infty \xi^j f_0(\eta) d\xi = F_j^+(\eta, b) + F_j^-(\eta, b). \tag{3.17}$$

$\mathcal{S}_i$ expanded to a lower series $O(\xi^4)$ and an upper series $O(B_z^4)$:

$$\int_{2k}^\infty \left(\frac{\xi^{r+i+1}}{1+\beta^2\xi^{2r-1}}\right)\frac{\partial f_0}{\partial \xi} d\xi \cong (r+i+1)F_{r+i}^+ - (3r+i)F_{3r+i-1}^+\beta^2 + (5r+i-1)F_{5r+i-2}^+\beta^4 \tag{3.18}$$

$$\int_0^{k/2} \left(\frac{\xi^{r+i+1}}{1+\beta^2\xi^{2r-1}}\right)\frac{\partial f_0}{\partial \xi} d\xi \Rightarrow \mathcal{S}_1 = \begin{pmatrix} \cdots & 2\frac{F_1^-}{\beta^2} - 3\frac{F_2^-}{\beta^4} + 4\frac{F_3^-}{\beta^6} & \cdots \\ \cdots & 3\frac{F_2^-}{\beta^2} - 4\frac{F_3^-}{\beta^4} & \cdots \\ \cdots & 4\frac{F_3^-}{\beta^2} & \cdots \end{pmatrix} \tag{3.19}$$

and similarly for $\mathcal{H}_{q,i}$,

$$\int_0^{k/2} \mu_q B_z \left(\frac{\xi^{2r+i+1/2}}{1+\beta^2\xi^{2r-1}}\right)\frac{\partial f_0}{\partial \xi} d\xi \Rightarrow$$

$$\mathcal{H}_1 = \begin{pmatrix} \cdots & \frac{3}{2}\frac{F_{1/2}^-}{\beta^2} - \frac{5}{2}\frac{F_{3/2}^-}{\beta^4} + \frac{7}{2}\frac{F_{5/2}^-}{\beta^6} - \frac{9}{2}\frac{F_{7/2}^-}{\beta^8} & \cdots \\ \cdots & \frac{5}{2}\frac{F_{3/2}^-}{\beta^2} - \frac{7}{2}\frac{F_{5/2}^-}{\beta^4} + \frac{9}{2}\frac{F_{7/2}^-}{\beta^6} & \cdots \\ \cdots & \frac{7}{2}\frac{F_{5/2}^-}{\beta^2} - \frac{9}{2}\frac{F_{7/2}^-}{\beta^4} & \cdots \end{pmatrix} \cdot \mu_q B_z \tag{3.20}$$

### 3.1.3 Classical electron gas approximation in a small magnetic field

When $\eta \leq -4$, the Fermi-Dirac distribution approaches the Boltzmann distribution. Under these conditions, the Fermi-Dirac integrals reduce to:

$$F_j(\eta) = \exp(\eta) \int_0^\infty \xi^j \exp(\xi) d\xi = \exp(\eta)\Gamma(j+1), \tag{3.21}$$

$$F_j^+(\eta, b) = \exp(\eta) \int_b^\infty \xi^j \exp(\xi) d\xi = \exp(\eta)\Gamma(j+1, b), \tag{3.22}$$

$$F_j^-(\eta, b) = \exp(\eta) \int_b^\infty \xi^j \exp(\xi) d\xi = \exp(\eta)[\Gamma(j+1) - \Gamma(j+1, b)], \tag{3.23}$$

where $\Gamma(j+1)$ and $\Gamma(j+1, b)$ are the complete and incomplete GAMMA functions, respectively.

The transport integrals reduce to

$$\begin{aligned} \mathcal{S}_i &= (\mathcal{S}_1)_{[2r+2,i+1]} + \\ &\exp(\eta) \sum_{n=0}^{\infty} (-1)^n [(2n+1)r + i - (n-1)] \beta^{2n} \Gamma([2n+1]r + i - [n-1], b), \end{aligned} \tag{3.24}$$

$$(\mathcal{S}_1)_{[2r+2,i+1]} = \begin{pmatrix} \cdots & \sum_{n=0}^{\infty}(-1)^n(n+2)(\frac{1}{\beta})^{2(n+1)}[\Gamma(n+2) - \Gamma(n+2,b)] & \cdots \\ \cdots & \sum_{n=1}^{\infty}(-1)^{(n+1)}(n+2)(\frac{1}{\beta})^{2n}[\Gamma(n+2) - \Gamma(n+2,b)] & \cdots \\ \cdots & \sum_{n=2}^{\infty}(-1)^n(n+2)(\frac{1}{\beta})^{2(n-2)}[\Gamma(n+2) - \Gamma(n+2,b)] & \cdots \end{pmatrix} \cdot \exp(\eta) \tag{3.25}$$

$$\begin{aligned} \mathcal{H}_{q,i} &= (\mathcal{H}_1)_{[2r+2,i+1]} + \\ &\mu_q B_z \exp(\eta) \sum_{n=0}^{\infty} \left[(2n+2)r + i + \frac{1}{2} - n\right] \beta^n \Gamma([2n+2]r + i + \frac{1}{2} - n, b), \end{aligned} \tag{3.26}$$

$$(\mathcal{H}_1)_{[2r+1,i+1]} =$$
$$\begin{pmatrix} \cdots & \sum_{n=0}^{\infty}(-1)^n(2n+3)(\frac{1}{\beta})^{2(n+1)}[\Gamma(n+\frac{3}{2})-\Gamma(n+\frac{3}{2},b)] & \cdots \\ \cdots & \sum_{n=1}^{\infty}(-1)^{(n+1)}(2n+3)(\frac{1}{\beta})^{2n}[\Gamma(n+\frac{3}{2})-\Gamma(n+\frac{3}{2},b)] & \cdots \\ \cdots & \sum_{n=2}^{\infty}(-1)^n(2n+3)(\frac{1}{\beta})^{2(n-2)}[\Gamma(n+\frac{3}{2})-\Gamma(n+\frac{3}{2},b)] & \cdots \end{pmatrix} \cdot \frac{\mu_q}{2} B_z \exp(\eta) \tag{3.27}$$

### 3.1.4 High-field approximation, $\beta^2 \to \infty$

An asymptotic series approximation of the transport integrals is calculated as $B_z$ is very large. The large $\beta^2$ condition makes this approximation also useful where there is very low scattering, e.g. at low temperatures in an ordered lattice or when the carrier mobility is high. The transport integrals to $O(1/B_z^2)$ are

$$\mathcal{S}_i = \frac{(-r+i+2)F_{-r+i+1}(\eta)}{\beta^2} \tag{3.28}$$

$$\mathcal{H}_{q,i} = \frac{(i+\frac{3}{2})F_{i+1/2}(\eta)}{\beta^2} \tag{3.29}$$

This approximation is important because the very-high magnetic field regime of quantum transport is known to approach the classical limit. [2] If we assume only closed orbits in reciprocal space for transport, we can predict the saturation behavior of the magnetoresistivity, thermopower, and electron thermal conductivity at very high fields.

This asymptotic approximation becomes invalid when the radius of the cyclotron orbits of the electrons is of the order of the deBroglie wavelength in the material. In this regime, this approximation yiels only qualitative results. The derivation given in § 2.5 is within the Boltzmann context and yields quantitative results for the high field classical limit.

# Chapter 4

# 2D Calculation of Transport Coefficients

## 4.1 Semiclassical calculation

### 4.1.1 Transport coefficients of a 2D layer in a uniform magnetic field in the $\hat{z}$-direction

The 2D semiclassical calculation shows the behavior of the transport coefficients at magnetic fields small enough so that quantum effects are not significant.[1]. The electronic dispersion relation for the quantum well is given by:

$$\varepsilon(k_x, k_y) = \frac{\hbar^2 {k_x}^2}{2m_x} + \frac{\hbar^2 {k_y}^2}{2m_y} + \frac{\hbar^2 \pi^2}{2m_z a^2}. \tag{4.1}$$

The transport integrals in the 2D case were calculated:

$$\mathcal{S}_i' = \int_0^\infty \frac{\xi^{r+i+1/2}}{1+\beta^2} \frac{\partial f_0^*}{\partial \xi} d\xi \tag{4.2}$$

$$\mathcal{H}_{q,i}' = \int_0^\infty \mu_q \frac{\xi^{2r+i} B_z}{1+\beta^2} \frac{\partial f_0^*}{\partial \xi} d\xi, \tag{4.3}$$

[1]These two-dimensional calculations hold the same constraints as the calculations in Chapter 3

where the constants are:

$$K' = \frac{2N_v \pi e \mu_x \sqrt{m_x m_y}}{h^2 a} k_B T \Lambda \tag{4.4}$$

$$K_1' = \frac{4N_v \pi \mu_x \sqrt{m_x m_y}}{h^2 a} k_B T^{3/2} \Lambda \frac{k_B}{e} \tag{4.5}$$

and

$$f_0^* = \frac{1}{\exp[\xi - (\eta - \varsigma_0)] + 1} \tag{4.6}$$

The 2D transport equations are calculated to be:

$$\sigma = K' \frac{{\mathcal{S}'_0}^2 + \mathcal{H}'_{x,0}\mathcal{H}'_{y,0}}{\mathcal{S}'_0} \tag{4.7}$$

$$\alpha = -\frac{k_B}{e}\left[\frac{\mathcal{S}'_0\mathcal{S}'_1 + \mathcal{H}'_{x,0}\mathcal{H}'_{y,1}}{{\mathcal{S}'_0}^2 + \mathcal{H}'_{x,0}\mathcal{H}'_{y,0}} - (\eta - \varsigma_0)\right] \tag{4.8}$$

$$\kappa = K_1'\left(\mathcal{S}_2' + \frac{\mathcal{S}_0'\mathcal{H}'_{x,1}\mathcal{H}'_{y,1} - 2\mathcal{H}'_{x,0}\mathcal{H}'_{y,1}\mathcal{S}_1' - \mathcal{S}_0'{\mathcal{S}_0'}^2}{{\mathcal{S}_0'}^2 + \mathcal{H}'_{x,0}\mathcal{H}'_{y,0}}\right), \tag{4.9}$$

where a is the thickness of the layer and

$$\varsigma_0 = \frac{\hbar^2\pi^2}{2m_z a^2}\frac{1}{k_B T}. \tag{4.10}$$

### 4.1.2 Small-field approximation, $\beta^2 \ll 1$

This case is similar to the 3D calculation (§3.1.3) and the approximations are the same. The following expressions were calculated for the and lower series, $O(\xi^5)$ and $O(\frac{1}{B_z^2})$, respectively.

$$\int_0^{k/2}\left(\frac{\xi^{r+i+1/2}}{1+\beta^2\xi^{2r-1}}\right)\frac{\partial f_0^*}{\partial \xi}d\xi \Rightarrow$$

$$\mathcal{S}_1 = \frac{1}{2}\cdot\begin{pmatrix} \cdots & 3\frac{F_{1/2}^-}{\beta^2} - 5\frac{F_{3/2}^-}{\beta^4} + 7\frac{F_{5/2}^-}{\beta^6} - 9\frac{F_{7/2}^-}{\beta^8} & \cdots \\ \cdots & 5\frac{F_{3/2}^-}{\beta^2} - 7\frac{F_{5/2}^-}{\beta^4} + 9\frac{F_{7/2}^-}{\beta^6} & \cdots \\ \cdots & 7\frac{F_{5/2}^-}{\beta^2} - 9\frac{F_{7/2}^-}{\beta^4} & \cdots \end{pmatrix} \tag{4.11}$$

$$\int_{2k}^{\infty}\left(\frac{\xi^{r+i+1/2}}{1+\beta^2\xi^{2r-1}}\right)\frac{\partial f_0^*}{\partial\xi}d\xi \Rightarrow \mathcal{S}_1$$
$$\cong \left(r+i+\frac{1}{2}\right)F^+_{3r+i+1/2} - \left(3r+i+\frac{1}{2}\right)F^+_{3r+i-1/2}\beta^2 + \left(5r+i-\frac{3}{2}\right)F^+_{5r+i-3/2}\beta^4 \tag{4.12}$$

$$\int_0^{k/2}\mu_q B_z\left(\frac{\xi^{2r+i}}{1+\beta^2\xi^{2r-1}}\right)\frac{\partial f_0^*}{\partial\xi}d\xi \Rightarrow$$
$$\mathcal{H}_1 = \begin{pmatrix} \cdots & \frac{F_0^-}{\beta^2} - 2\frac{F_1^-}{\beta^4} + 3\frac{F_2^-}{\beta^6} - 4\frac{F_3^-}{\beta^8} & \cdots \\ \cdots & 2\frac{F_1^-}{\beta^2} - 3\frac{F_2^-}{\beta^4} + 4\frac{F_3^-}{\beta^6} & \cdots \\ \cdots & 3\frac{F_2^-}{\beta^2} - 4\frac{F_3^-}{\beta^4} & \cdots \end{pmatrix}\cdot\mu_q B_z \tag{4.13}$$

$$\int_{2k}^{\infty}\mu_q B_z\left(\frac{\xi^{2r+i}}{1+\beta^2\xi^{2r-1}}\right)\frac{\partial f_0^*}{\partial\xi}d\xi \cong \mu_q B_z\left[(2r+i)F^+_{2r+i-1} - (4r+i-1)F^+_{3r+i-2}\beta^2\right] \tag{4.14}$$

### 4.1.3 Classical electron gas in a magnetic field

The results here are also similar to the 3D case, also as a result of the Fermi-Dirac distribution approaching the Boltzmann distribution. Using the same Fermi-Dirac integrals in terms of GAMMA functions, we have:

$$\begin{aligned}\mathcal{S}_i &= (\mathcal{S}_1)_{[2r+2,i+1]} + \exp(\eta)\cdot \\ &\quad \sum_{n=0}^{\infty}(-1)^n\left[(2n+1)r+i-\left(n-\frac{1}{2}\right)\right]\beta^{2n}\Gamma([2n+1]r+i-\left[n-\frac{1}{2}\right],b)\end{aligned} \tag{4.15}$$

$$(\mathcal{S}_1)_{[2r+2,i+1]} =$$
$$\begin{pmatrix} \cdots & \sum_{n=0}^{\infty}(-1)^n(2n+3)\left(\frac{1}{\beta}\right)^{2(n+1)}\left[\Gamma(n+\frac{3}{2}) - \Gamma(n+\frac{3}{2},b)\right] & \cdots \\ \cdots & \sum_{n=1}^{\infty}(-1)^{n+1}(2n+3)\left(\frac{1}{\beta}\right)^{2n}\left[\Gamma(n+\frac{3}{2}) - \Gamma(n+\frac{3}{2},b)\right] & \cdots \\ \cdots & \sum_{n=2}^{\infty}(-1)^n(2n+3)\left(\frac{1}{\beta}\right)^{2(n-2)}\left[\Gamma(n+\frac{3}{2}) - \Gamma(n+\frac{3}{2},b)\right] & \cdots \end{pmatrix}\cdot\exp(\eta)$$

(4.16)

$$\mathcal{H}_{q,i} = (\mathcal{H}_1)_{[2r+2,i+1]} + \mu_q B_z \exp(\eta) \cdot \sum_{n=0}^{\infty} (-1)^n (n+1) \left(\frac{1}{\beta}\right)^{2(n+1)} [(2n+2)r + i - n] \beta^n \Gamma([2n+2]r + i - n, b) \tag{4.17}$$

$$(\mathcal{H}_1)_{[2r+2,i+1]} = \begin{pmatrix} \cdots & \sum_{n=0}^{\infty}(-1)^n(n+1)\left(\frac{1}{\beta}\right)^{2(n+1)}[\Gamma(n+1) - \Gamma(n+1,b)] & \cdots \\ \cdots & \sum_{n=1}^{\infty}(-1)^{n+1}(n+1)\left(\frac{1}{\beta}\right)^{2n}[\Gamma(n+1) - \Gamma(n+1,b)] & \cdots \\ \cdots & \sum_{n=2}^{\infty}(-1)^n(n+1)\left(\frac{1}{\beta}\right)^{2(n-2)}[\Gamma(n+1) - \Gamma(n+1,b)] & \cdots \end{pmatrix} \cdot \frac{\mu_q B_z}{2} \exp(\eta) \tag{4.18}$$

# Chapter 5

# The Figure of Merit Under Landau-Level Quantization

## 5.1 Quantization of Orbits in the Semiclassical Framework: Transport Coefficients in the Absence of Landau-level Broadening

Transport in the Landau level regime is due to the hopping of carriers from one orbit to another due to a collision which changes the wavevector. Collisions are governed by a mean lifetime in a particular orbit and is the same as the relaxation time in the absence of a magnetic field. Cases which involve high disorder are treated using percolation theory for transport. We will only concern ourselves only with the case of weak disorder and single-electron transport with no many-body effects, which result only in Landau-level broadening as a result of carrier lifetime broadening.

The change in wavevector is influenced by the electric field. In this electric field a potential exists across the material, which produces a net drift velocity $u_x$ which can be viewed as a diffusion of orbital centers. In this manner, we can apply the Boltzmann equation as a first approximation to calculate the transport coefficients.

Here, we assume transport in the x-y plane and carrier and heat currents in the $\hat{x}$-direction and magnetic field in the $\hat{z}$-direction. In this first approximation we assume

that the Landau-levels and its associated density of states $g(E)$ remain as sharp $\delta$-functions and are not broadened by scattering.

$$g(E) = g_0\,\delta(E - E_N) \tag{5.1}$$

where $E_N$ are the energies of the Landau levels, ignoring the effects of spin,

$$E_N = \left(N + \frac{1}{2}\right)\hbar\omega_c, \tag{5.2}$$

and

$$g_0 = \frac{1}{2\pi l^2} \tag{5.3}$$

where where $l$ is the classical orbital radius of the electron and $l^2 = \hbar/eB$. Substituting into Equation ??, the electron and heat currents are given by,

$$\begin{aligned} j_x &= e\int_0^\infty dE\,\frac{\partial f_0}{\partial E}\,u_x^2\cdot \\ &\quad \sum_N\left\{g_0\,\delta(E-E_N)\frac{-\tau}{1+(\omega_c\tau)^2}\left[(1-\omega_c\tau)\frac{\partial\zeta}{\partial x}+\left(\frac{E-\zeta}{T}\right)\frac{\partial T}{\partial x}\right]\right\} \end{aligned} \tag{5.4}$$

$$\begin{aligned} w_x &= -\int_0^\infty dE\,\frac{\partial f_0}{\partial E}\,u_x^2\,(E-\zeta)\cdot \\ &\quad \sum_N\left\{g_0\,\delta(E-E_N)\frac{-\tau}{1+(\omega_c\tau)^2}\left[(1+\omega_c\tau)\frac{\partial\zeta}{\partial x}+\left(\frac{E-\zeta}{T}\right)\frac{\partial T}{\partial x}\right]\right\}. \end{aligned} \tag{5.5}$$

With the relaxation time is dependent on energy, $\tau = \tau(E)$, we integrate both expressions. These reduce to,

$$j_x = -e\,g_0\sum_N\left\{\left.\frac{\partial f_0}{\partial E}\right|_{E_N} u_N^2\frac{\tau_N}{1+(\omega_c\tau_N)^2}\left[(1-\omega_c\tau_N)\frac{\partial\zeta}{\partial x}+\left(\frac{E_N-\zeta}{T}\right)\frac{\partial T}{\partial x}\right]\right\}, \tag{5.6}$$

$$w_x = g_0 \sum_N \left\{ \left.\frac{\partial f_0}{\partial E}\right|_{E_N} u_N^2 (E_N - \zeta) \frac{\tau_N}{1 + (\omega_c \tau_N)^2} \left[ (1 + \omega_c \tau_N) \frac{\partial \zeta}{\partial x} + \left( \frac{E_N - \zeta}{T} \right) \frac{\partial T}{\partial x} \right] \right\}, \tag{5.7}$$

where $\tau_N = \tau(E_N)$ and $u_N = u_x(E_N)$.

Physically, it is necessary to maintain constant carrier density given by

$$N_s = \int_0^\infty f_0 \, g(E) \, dE. \tag{5.8}$$

This implies a Fermi energy which oscillates with with increasing magnetic field.

$$E_f = E_n - k_B T \ln \left( \frac{g_0}{N} \right), \tag{5.9}$$

for $g_0 \gg 1$.

In calculating the isothermal conductivity, remember that $\nabla T = 0$. The conductivity in the $\hat{x}$-direction is given by,

$$\sigma_x = \frac{j_x}{\mathcal{E}_x} = j_x / \frac{\partial \zeta}{\partial x} \frac{1}{e}. \tag{5.10}$$

Substituting into Equations 5.6 & 5.10, we find

$$\sigma_x = -e^2 g_0 \sum_N \left. \frac{\partial f_0(\zeta = E_f)}{\partial E} \right|_{E_N} \tau(E_N) u_N^2. \tag{5.11}$$

The Seebeck coefficient is calculated using the $i_y = 0$, where

$$i_y = -e g_0 \sum_N \left\{ \left.\frac{\partial f_0}{\partial E}\right|_{E_N} u_N^2 \frac{\tau_N}{1 + (\omega_c \tau_N)^2} \left[ (1 + \omega_c \tau_N) \frac{\partial \zeta}{\partial x} + \left( \frac{E_N - \zeta}{T} \right) \frac{\partial T}{\partial x} \right] \right\} \tag{5.12}$$

is calculated similarly to $i_x$. The Seebeck coefficient simplifies to

$$\alpha = -\frac{1}{eT} \frac{\sum_N \left. \frac{\partial f_0(\zeta = E_f)}{\partial E} \right|_{E_N} (E_N - \zeta) u_N^2 (1 + \omega \tau(E_N))}{\sum_N \left. \frac{\partial f_0}{\partial E} \right|_{E_N} (1 + (\omega_c \tau_N)^2) u_N^2}. \tag{5.13}$$

The thermal conductivity is

$$\kappa = \frac{g_0}{T}\sum_N \left.\frac{\partial f_0(\zeta = E_f)}{\partial E}\right|_{E_N} (E_N - \zeta)^2 \tau(E_N) \left[\frac{e\alpha T}{E_N - \zeta} - \frac{1}{1+\omega_c^2\tau^2}\right] u_N^2. \qquad (5.14)$$

## 5.2 Calculations with the Self-Consistent Born Approximation

The self-consistent Born approximation yields a semi-elliptical density of states. The calculation is reviewed by Ando et al. [1][pp.536-540]. The total Hamiltonian can be divided into a ground state Hamiltonian which is essentially a quantum mechanical harmonic oscillator and the scattering Hamiltonian in the number representation formalism:

$$H = H^{(0)} + H^{(1)}, \qquad (5.15)$$

and

$$H^{(0)} = \frac{1}{2m}(\mathbf{p} + e\mathbf{A})^2 = \sum_{NX} E_N a_{NX}^+ a_{NX}, \qquad (5.16)$$

$$\begin{aligned} H^{(1)} &= \sum_i \sum_\nu v^{(\nu)}(\vec{r} - \vec{r}_i, z_i) \\ &= \sum_i \sum_\nu \sum_{NX} \sum_{N'X'} \langle NX|v^{(\nu)}(\vec{r} - \vec{r}_i, z_i)|N'X'\rangle a_{NX}^+ a_{N'X'}, \end{aligned} \qquad (5.17)$$

For simplicity, we assume only elastic scattering by short-range scatterers. Scattering by a potential in which interaction occurs only at a short-range is given by a range $d$ such that $d < l/(2N+1)^{1/2}$. In the calculation of the thermomelectric figure of merit, the temperature range of concern is of the order of room temperature ($\sim 300K$). This is a practical consideration for effective thermoelectric refrigeration. In this temperature range, the primary scattering mechanism is due to phonons. In the following calculations we assume elastic scattering.

Within the Green's function formalism, level broadening in the density of states is solved self-consistently. The formulation leads to a semi-elliptical form of the density

of states given by,

$$g(E) = \frac{1}{2\pi l^2} \sum_N \left[1 - \left(\frac{E - E_N}{\Gamma^2}\right)^2\right]^{1/2}. \tag{5.18}$$

A problem arises when we attempt to consider contributions to transport at the spectral edges of the Landau levels. The unphysically sharp cutoff of the density of states does not permit contributions of extended states between Landau-levels and also causes computational errors in the numerical calculations.

An alternative formulation uses the path integral method in calculating the density of states. This leads to a Gaussian form of the density of states given by,

$$g(E) = \frac{1}{2\pi l^2} \sum_N \left(\frac{\pi}{2}\Gamma^2\right)^{-1/2} \exp\left(-2\frac{(E - E_N)^2}{\Gamma^2}\right). \tag{5.19}$$

The Landau-level broadening is given by

$$\Gamma^2 = \frac{2\hbar}{\pi\tau_f}\hbar\omega_c. \tag{5.20}$$

This broadening is inversely proportional to the relaxation time $\tau$. In the review given by Ando et. al [1], constant isotropic relaxation time was assumed. At low magnetic fields, the common energy-dependent functional expression for $\tau$ is given by [4]

$$\tau(E) = \tau_0 E^{r-1/2} \tag{5.21}$$

in the context of the semiclassical approximation. Under Landau-level quantization of carriers it seems sensible to attempt a magnetic field dependent relaxation of the same form,

$$\tau(E, \omega_c) = \tau_0 (E + \hbar\omega_c/2)^{r-1/2}. \tag{5.22}$$

This functional form is consistent with the correspondence principle in that at semi-classical values of magnetic field, Equation 5.21 reduces to Equation /refeqn:tauQuant. At high magnetic fields, this puts an upper limit to the relaxation time by translating the zeroth energy to $\hbar\omega_c$, the energy of the ground state Landau-level.

### 5.2.1 Conductivity

The diagonal conductivity calculated by the application of Kubo's center migration theory [10] and the use of the semielliptical density of states yields,

$$\sigma_{xx} = -\frac{e^2\hbar}{\pi L^2}\int dE\,\frac{\partial f_0}{\partial E}\sum_{NX}\langle 0|a_{NX}X\left(\Im\frac{1}{E-\mathcal{H}}\right)\dot{X}\left(\Im\frac{1}{E-\mathcal{H}}\right)a^{+}_{NX}|0\rangle, \qquad (5.23)$$

where,

$$\begin{aligned}\dot{X} &= \frac{1}{i\hbar}[X,\mathcal{H}] \\ &= \frac{1}{\hbar}\sum_{\mu,i}\sum_{NX}\sum_{N'X'}\left(NX|l\frac{\partial v^{(\mu)}(\mathbf{r}-\mathbf{r_i},z_i)}{\partial y}|N'X'\right)a^{+}_{NX}a_{N'X'}, \qquad (5.24)\end{aligned}$$

reduces to

$$\sigma_{xx} = -\frac{e^2}{\pi^2\hbar}\int dE\,\frac{\partial f_0}{\partial E}(N+1/2)\left[1-\left(\frac{E-E_N}{\Gamma}\right)^2\right], \qquad (5.25)$$

for strong magnetic fields ($\omega_c\tau > 1$) and short-range scatterers.

In using the Gaussian density of states,

$$\sigma_{xx} = -\frac{e^2}{\pi^2\hbar}\int dE\,\frac{\partial f_0}{\partial E}(N+1/2)\left(\frac{2}{\pi}\right)^{1/2}\Gamma\exp\left[\frac{-2(E-E_N)}{\Gamma}\right], \qquad (5.26)$$

### 5.2.2 Seebeck Coefficient

The Seebeck coefficient or thermopower is calculated from the zero temperature conductivity $\sigma^{(0)}$. Here, we assume only elastic scattering by short-range scatterers. The zero temperature diagonal conductivity is given by,

$$\sigma^{(0)}_{xx} = (N+1/2)\frac{e^2}{\pi^2\hbar}\left[1-\left(\frac{E-E_N}{\Gamma}\right)^2\right]. \qquad (5.27)$$

The off-diagonal zero temperature conductivity is

and the diagonal Seebeck coefficient is then,

$$\alpha_{xx} = \frac{1}{eT}\int dE\,\frac{\partial f_0}{\partial E}(E-\zeta)\,\sigma^{(0)}_{xy} \qquad (5.28)$$

### 5.2.3 Electronic Thermal Conductivity

The thermal conductivity is given by

$$\kappa = \frac{1}{e^2 T} \int dE \, \frac{\partial f_0}{\partial E} (E - \zeta)^2 \, \sigma_{xx}^{(0)} \tag{5.29}$$

## 5.3 Carrier Dumping

Under Landau level quantization conditions, carrier dumping occurs in multiple pocket materials at sufficiently high magnetic fields. The electron density of pockets with lighter cyclotron effective mass $m_c^*$ is transferred to pockets with higher cyclotron effective mass. This occurs when the Landau level separation of the light mass pockets become larger than separations of the heavier mass pocket. This dumping occurs because the chemical potential is pinned to the closest Landau level.

The cyclotron effective mass is dependent on the effective mass tensor $\overleftrightarrow{\mathbf{m}}$ and the orientation of the magnetic field:

$$m_c^* = \left( \frac{\det(\overleftrightarrow{\mathbf{m}})}{\hat{b} \cdot \overleftrightarrow{\mathbf{m}} \cdot \hat{b}} \right)^{1/2}, \tag{5.30}$$

where $\hat{b}$ is the unit-vector of the magnetic field relative to the axis of the ellipsoid.

This transfer of carriers is useful in increasing the figure of merit because by orienting the magnetic field in a specified direction, carriers from pockets with lesser contributions to the figure of merit can be transferred to pockets which have higher contributions. According to Hicks [8][p.5], the ellipsoid oriented with the highest value of $\mu(m_{e1} m_{e2}$ gives the highest figure of merit. In the two dimensional case under a quantizing magnetic field, this translates to the pockets with the highest value of $\mu m_c^*$.

In the reduction of the dimensionality of the carriers, several things occur. Assuming a two-dimensional transport in the $\hat{x}$-$\hat{y}$ directions, bound states are formed in

the $\hat{z}$ direction such that

$$\frac{k_z^2}{2m_z} = \frac{N\pi^2}{2m_z a^2}. \tag{5.31}$$

From the definition of effective mass,

$$\frac{1}{m_\perp} = \frac{\partial^2 E}{\partial k_\perp^2}\frac{1}{\hbar^2} \tag{5.32}$$

where $\perp$ are the perpendicular components to the 2D plane. We can see that as $k_z$ approaches the bound state constant value, the perpendicular component of the effective mass becomes infinite.

Unlike in 3D, the effect of the application of a magnetic field depends only on the perpendicular component of the field to the plane. The effect is given by

$$B_{eff} = \hat{n}_\perp \cdot \vec{B} \tag{5.33}$$

which means that any angular variation of the magnetic to the perpendicular unit vector $\hat{n}_\perp$ is just the equivalent to a change in magnitude of the magnetic field. Thus, the application of a magnetic field always means in the direction perpendicular to the 2D surface.[1]

This has several implications for carrier dumping. Carrier dumping should not occur for high symmetry Fermi surfaces for the following reasons. For example, assuming the high symmetry surface shown in Figure 5-1, a cut along the x-y plane would result in a Fermi curve consisting of 4 ellipses and one circle shown in Figure ??. This cut with result in inequivalent ellipses. The carrier then dump into the lower energy pockets. The full pockets then become their own set of symmetrical Fermi curves.

[1]We assume that the magnetic field is low enough so that magnetic breakdown does not occur across the bound states in the $\hat{z}$-direction.

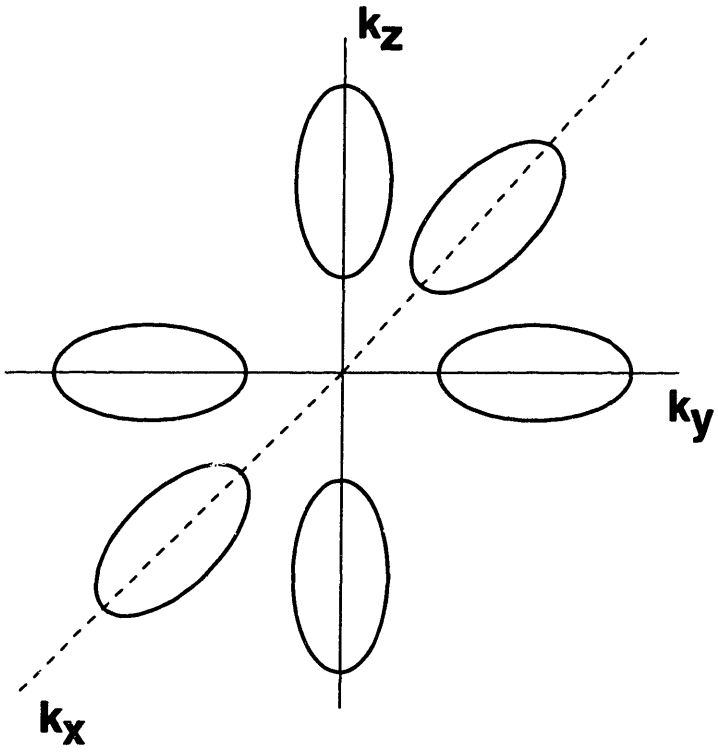


Figure 5-1: Hypothetical Fermi surface with high symmetry.

# Chapter 6

# Numerical Results For Thermoelectric Materials

## 6.1 Bismuth

The bismuth rhombohedral lattice can be expressed as a hexagonal unit cell with lattice constants: $a_0 = 4.5\mathring{A}$, $c_0 = 11.9\mathring{A}$. The carriers are distributed in 3 electron pockets and 1 hole pocket. The electron pockets consist of ellipsoidal surfaces located at the L points of the Brillouin zone. The hole pocket is a single ellipsoidal surface at the T point. [8][p.4].

When transport occurs in three dimensions, there is an overlap between the electron and hole bands. This overlap has an energy of 0.038 eV. This overlap results in mixed carrier transport with approximately equal electron and hole carrier densities. Hicks [8][p.5] calculates that the electron and hole bands uncross at about $300\mathring{A}$. This separation effectively transforms the material into a single-band system. Thus, we can treat the two-dimensional system as consisting of only electron carriers.

The 3 electron pockets are oriented 120° to each other (Figure 6-1). The principal

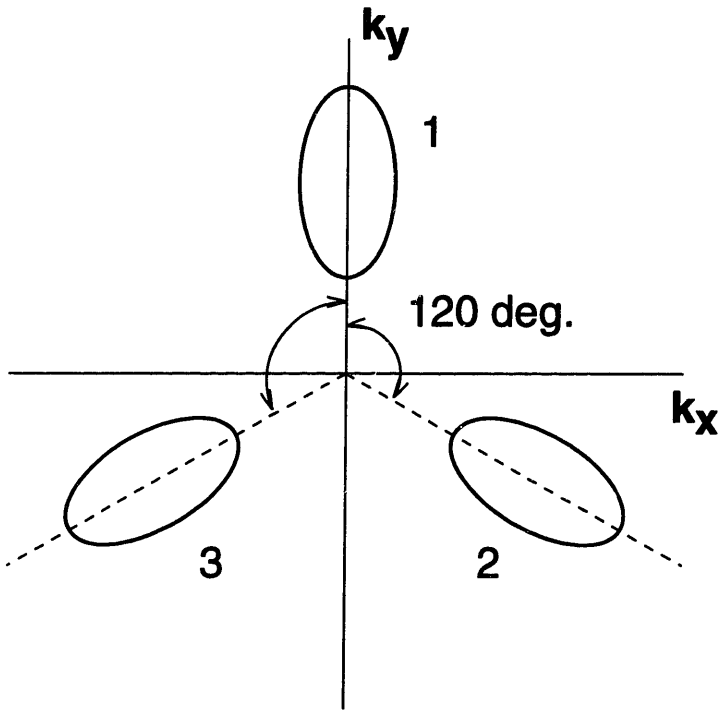


Figure 6-1: The three ellipsoidal electron pockets of Bi are oriented 120° to each other, centered at $\mathbf{k} = (0, 0, 0)$.

effective mass tensor is given by

$$\overleftrightarrow{\mathbf{m}} = \begin{pmatrix} 0.00651 & 0 & 0 \\ 0 & 1.362 & 0 \\ 0 & 0 & 0.00993 \end{pmatrix} \cdot m_0. \tag{6.1}$$

and the mobility components are given as

$$\overleftrightarrow{\mu} = \begin{pmatrix} 3.5 & 0 & 0 \\ 0 & 0.034 & 0 \\ 0 & 0 & 1.4 \end{pmatrix} (\text{in } m^2 V^{-1} s^{-1}). \tag{6.2}$$

### 6.1.1 Carrier Dumping

In Figure 6-1, the electron pockets are shown in the x-z plane. If we apply a magnetic field in the $\hat{z}$-direction, the field aligns with the principal axis of ellipsoid 1. The

cyclotron effective mass of ellipsoid 1 is calculated from Equation 5.30 as

$$m_c^*1 = (m_{11}m_{22})^{1/2}, \tag{6.3}$$

and $\hat{b}_1 = (0, 0, 1)$.

The other ellipsoids (2 and 3) have the same cyclotron effective mass:

$$m_{c2}^* = \left(\frac{m_{11}m_{22}m_{33}}{m_{11}\sin^2\theta + m_{33}\cos^2\theta}\right)^{1/2}. \tag{6.4}$$

For $Bi_2Te_3$, $\theta = 120°$ and $\hat{b}_2 = \hat{b}_3 = (\sin\theta, 0, \cos\theta)$.

## 6.2 Bismuth Telluride

### 6.2.1 Results of the Semiclassical Calculation

The semiclassical calculations for $Bi_2Te_3$ assumes six identical ellipsoids in a magnetic field, each contributing an equal amount to the transport. The orientation and any tilts of the ellipsoids are not taken into account. For low fields ($\omega\tau \lesssim 1$), quantitative results are in fair agreement with experiment. For higher fields, only qualitative results can be expected because the effects of Landau level quantization are not included. At fields where the $N = 0$ Landau level is much greater than the Fermi energy, the behavior of the transport coefficients are expected to approach the classical limit. The classical electron case (with $\eta = -4$) is used as a test case for the semiclassical calculation because it allows several simplifying approximations. In practice, carrier densities this low ($N \sim 10^{13}m^{-2}$) for 2D) are difficult to achieve in semiconductors because intrinsic carrier densities are higher than this value.

#### Three Dimensional Transport

The transport coefficients were calculated by direct numerical integration of the transport integrals (Equations 3.2 and 3.3 for the classical electron gas case, i.e. non-degenerate. The magnetic field is in the $\hat{z}$-direction of the principal axes of the

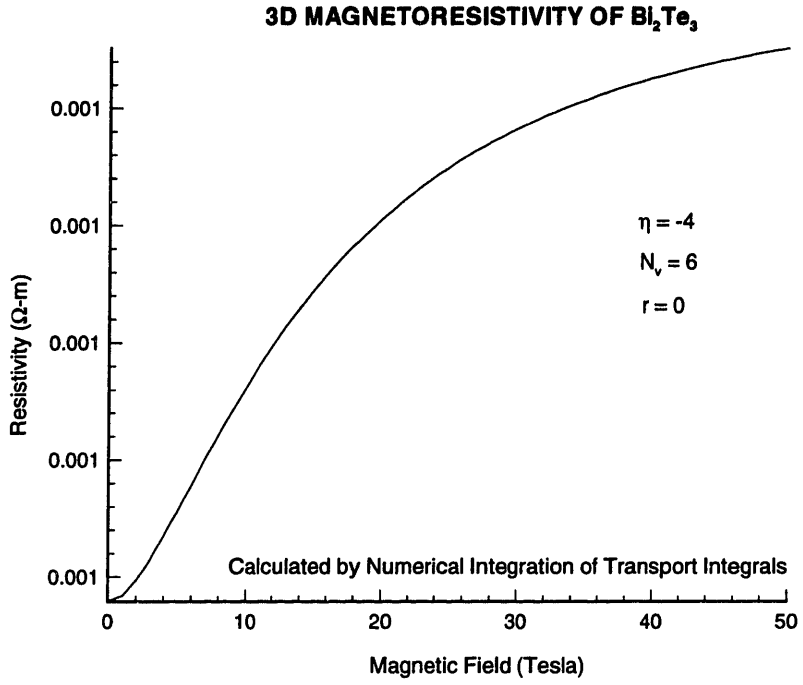


Figure 6-2: The resistivity $\rho_{xx}$ of $Bi_2Te_3$ shows saturation behavior at high magnetic fields. The scattering parameter $r = 0$ and the reduced Fermi energy $\eta = -4$.

ellipsoidal surfaces. The scattering parameter $r = 0$ is the value commonly used for $Bi_2Te_3$ [4][p.92][1]

Figure 6-2 shows the resistivity of $Bi_2Te_3$ in the direction perpendicular to the magnetic field along the highest mobility direction. At the reduced Fermi energy of $\eta = -4$, the electron gas is non-degenerate. A saturation behavior is apparent at high magnetic fields. From Equations 3.28 and 3.29, this saturation is proportional to $\beta^{-2} = (\mu_x B_z)^{-2}$. It is also expected that the saturation is sensitive $\eta$ such that as $\eta \ll -4$, the resistivity saturates more sharply and at lower fields.

The magnetic field dependence of the Seebeck coefficient, or thermopower, is shown in Figure 6-3; $\alpha_{xx}$ is along the same direction as $\rho_{xx}$. No saturation apparent up to 50 Tesla. This can be explained by the sensitivity of the thermopower to /*eta*; at values of $\eta \ll 0$, it can be expected that saturation does not occur until very high fields are reached ($> 100T$).

[1]Goldsmid defines the energy dependence of $\tau \propto E^r$. In this thesis, $\tau \propto E^{r-1/2}$. Thus, Goldsmid's $r = -0.5$ is equivalent to my $r = 0$.

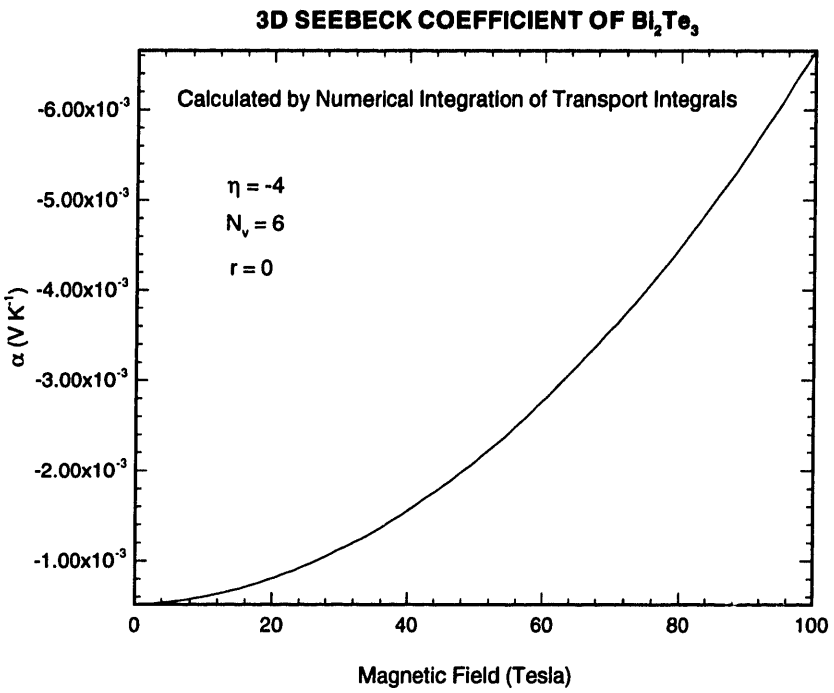


Figure 6-3: The magnetic field dependence of the Seebeck coefficient $\alpha_{xx}$ is shown. The scattering parameter $r = 0$ and the reduced Fermi energy $\eta = -4$.

From Figure 6-4, we find that at non-degenerate values of $\eta$, the contribution of the electrons ($\sim 10^{-3}W/m^2$) to the total thermal conductivity in $Bi_2Te_3$ is very small relative to the lattice contribution $\kappa_{ph} = 1.5W/m^2$. In the non-degenerate case, the electron thermal conductivity is negligible and the limiting value of the thermal conductivity becomes $\kappa_{ph}$. $\kappa_{xx}$ along the direction of $\sigma_{xx}$ also shows a saturation occurs at the same fields as $\rho_{xx}$. This behavior is consistent with the Wiedemann-Franz law.[2]

In Figure 6-5, ZT rises monotonically with no saturation up to 50 Tesla. The zero field value of ZT is rather small because $\eta = -4$ is not at the optimized value. However, we can see the sensitivity of ZT to a magnetic field for this non-degenerate case. Although it is impractical to maintain magnetic fields of 50 Tesla for refrigeration purposes, it is useful to know that an increase is possible over the bulk experimental value of 0.67 ?? for zero-field at a non-optimized value of $\eta$.

[2]The Wiedemann-Franz law states that $\rho_{xx} \propto \kappa_{xx}^{-1}$.

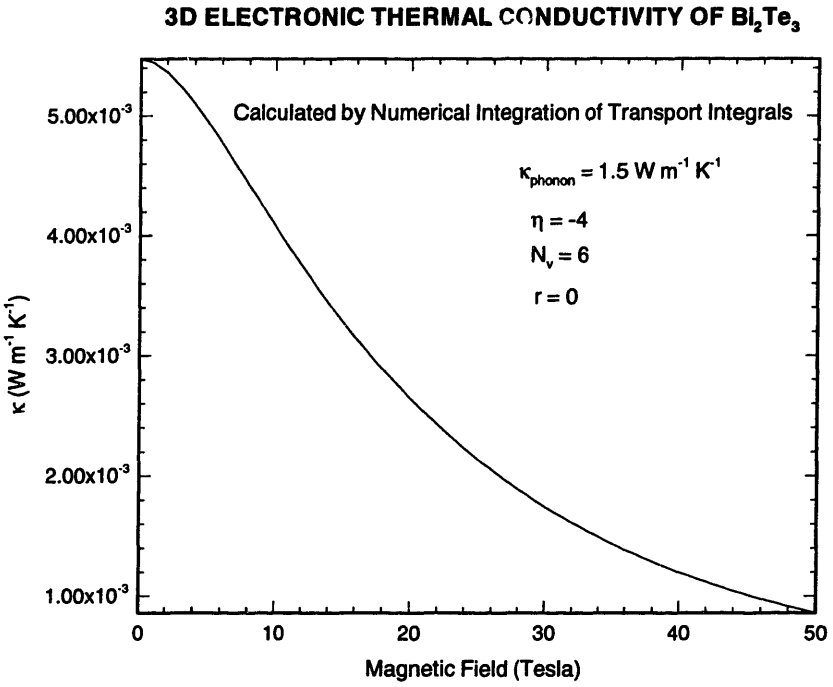


Figure 6-4: The electron contribution to the thermal conductivity $\kappa_{xx}$ as a function of magnetic field is shown. The scattering parameter $r = 0$ and the reduced Fermi energy $\eta = -4$.

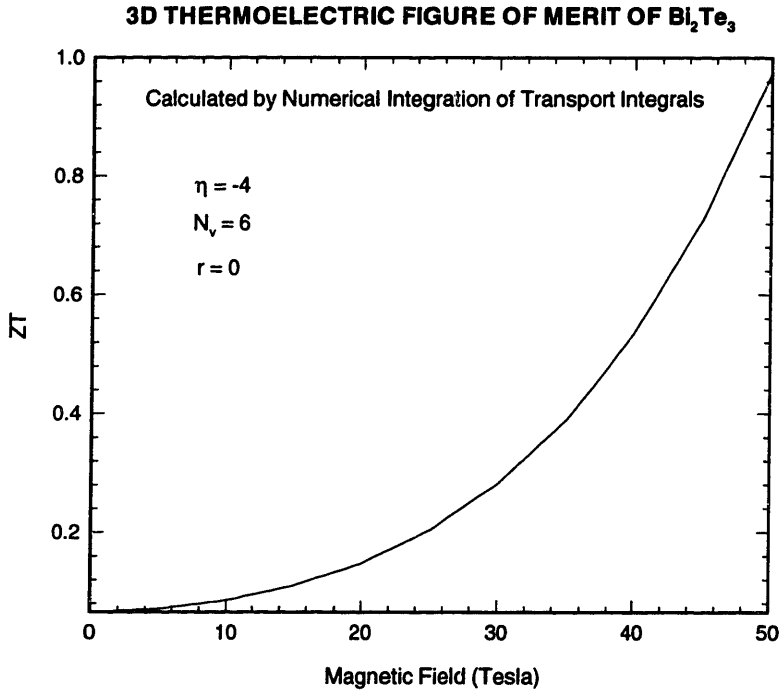


Figure 6-5: The thermoelectric figure of merit normalized to temperature $ZT$ is shown to rise monotonically up to 50 Tesla. The scattering parameter $r = 0$ and the reduced Fermi energy $\eta = -4$.

**Two-Dimensional Transport**

The transport coefficients were calculated for two-dimensional density of states by the direct numerical integration of the transport integrals given in Equations 4.2 and 4.3. This calculation is expected to be valid only for the low-field case ($\omega_c\tau \lesssim 1$). However, we can expected qualitative results which are related to the peak values of the diagonal resistivity $rho_{xx}$. In the high-field case, where $\omega_c\tau \gg 1$ and $\hbar\omega_c \gg k_BT$, $\sigma_{xx} = 0$ and subsequently $\rho_{xx} = 0$. So, the results for the high field case in the derivation in § 4.1 are dubious for the high field case. It is necessary to derive the high field case in the context of the Ziman calculation presented in § 2.5.

The results are given for the non-degenerate case with the reduced Fermi energy $\eta = -4$. The magnetic is applied in the $\hat{z}$-direction with respect to the principal axes of the ellipsoids. As in the 3D case, $r = 0$ is the value used for the scattering parameter.

The same values are used for the parameters $N_v$, $\eta$ and $r$ as in the three dimensional case.

The results are similar to the three-dimensional case. However, the values of ZT for $\eta = -4$ and thickness $a = 1000\mathring{A}$ yields a much lower figure of merit. This realizes the need to find the optimum value of $\eta$ in order to maximize ZT at each value of magnetic field.

### 6.2.2 Results from the Born-Approximation for Semi-Elliptical Density of States

The calculation of diagonal conductivity $\sigma_{xx}$ using a semi-elliptical density of states, requires that the Landau-levels be well separated such that $\hbar\omega_c \gg k_BT$. This means that no inter-Landau level scattering occurs. The Landau-level separation goes as

$$\hbar\omega_c \sim 10^{-4}\frac{B}{m_c^*/m_0} \qquad \text{(in eV)} \tag{6.5}$$

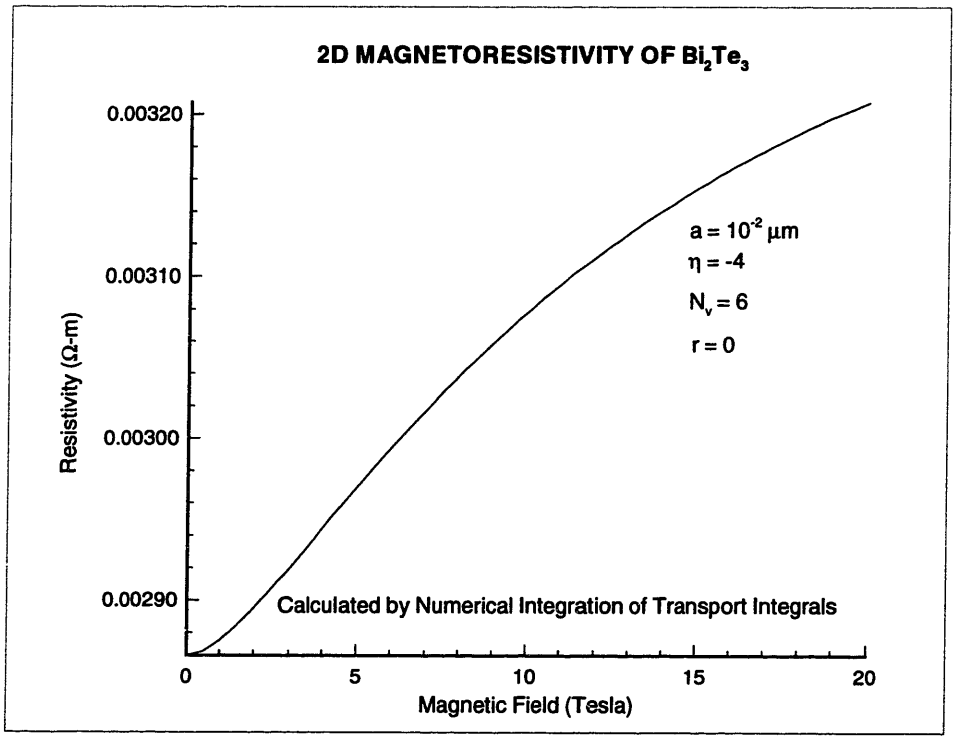


Figure 6-6: The dependence of the diagonal resistivity $\rho_{xx}$ on magnetic field is shown. $N_v = 6$ valleys with equal contributions are assumed. The scattering parameter $r = 0$ and the reduced Fermi energy $\eta = -4$. The thickness of the film is $100\mathring{A}$.

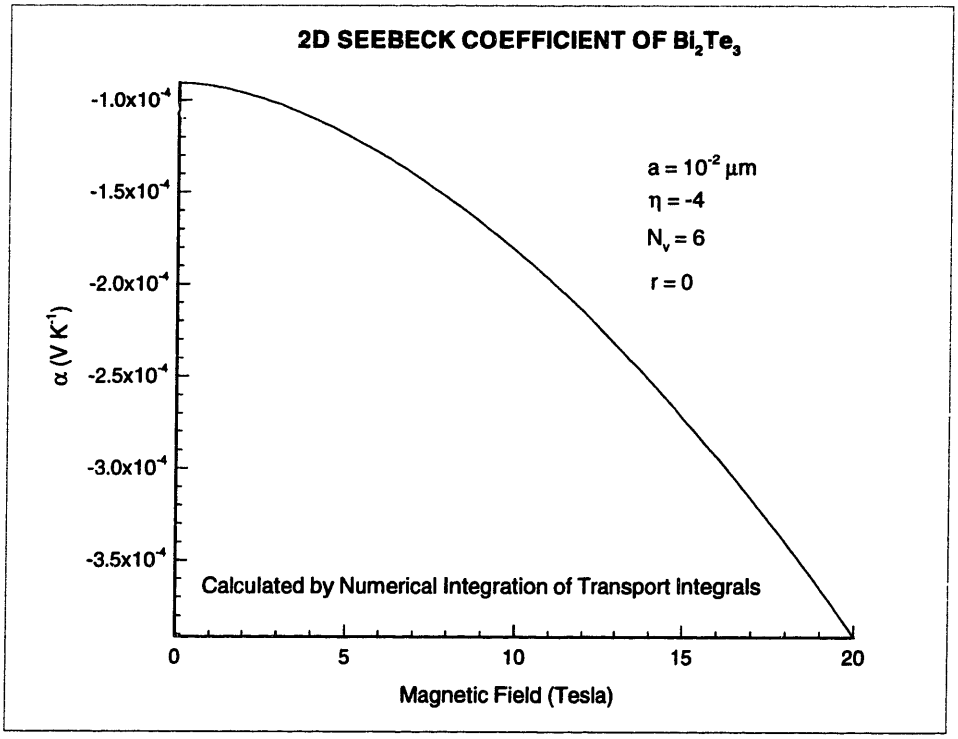


Figure 6-7: The dependence of the diagonal thermopower $\alpha_{xx}$ on magnetic field is shown. $N_v = 6$ valleys with equal contributions are assumed. The scattering parameter $r = 0$ and the reduced Fermi energy $\eta = -4$. The thickness of the film is $100\mathring{A}$.

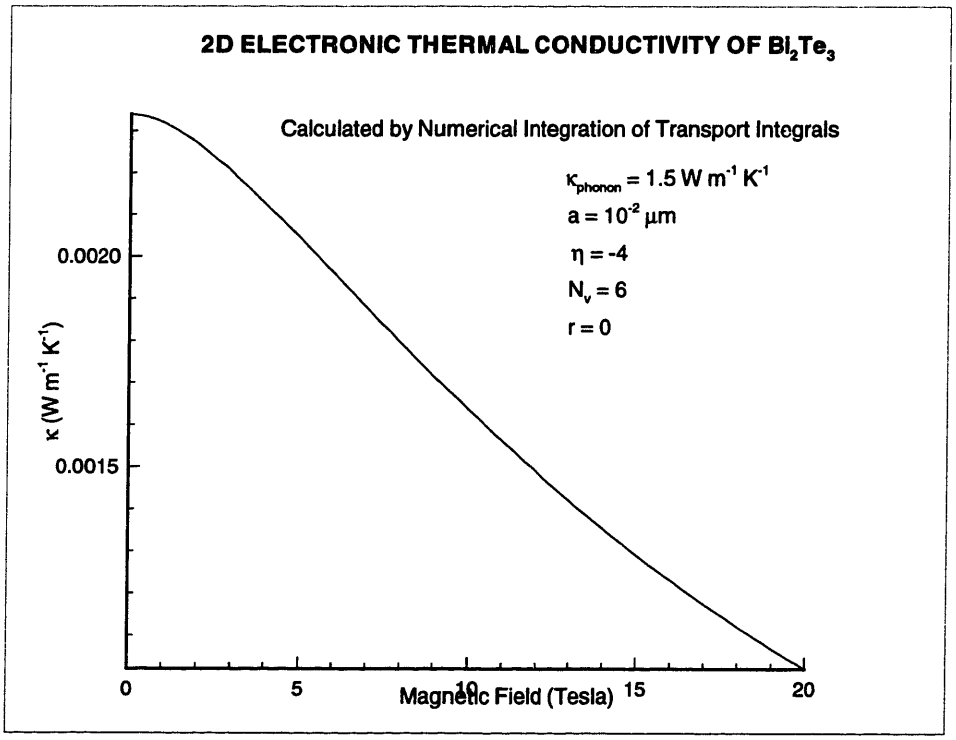


Figure 6-8: The dependence of the diagonal electron thermal conductivity $\kappa_{xx}$ on magnetic field is shown. $N_v = 6$ valleys with equal contributions are assumed. The scattering parameter $r = 0$ and the reduced Fermi energy $\eta = -4$. The thickness of the film is $100\mathring{A}$.

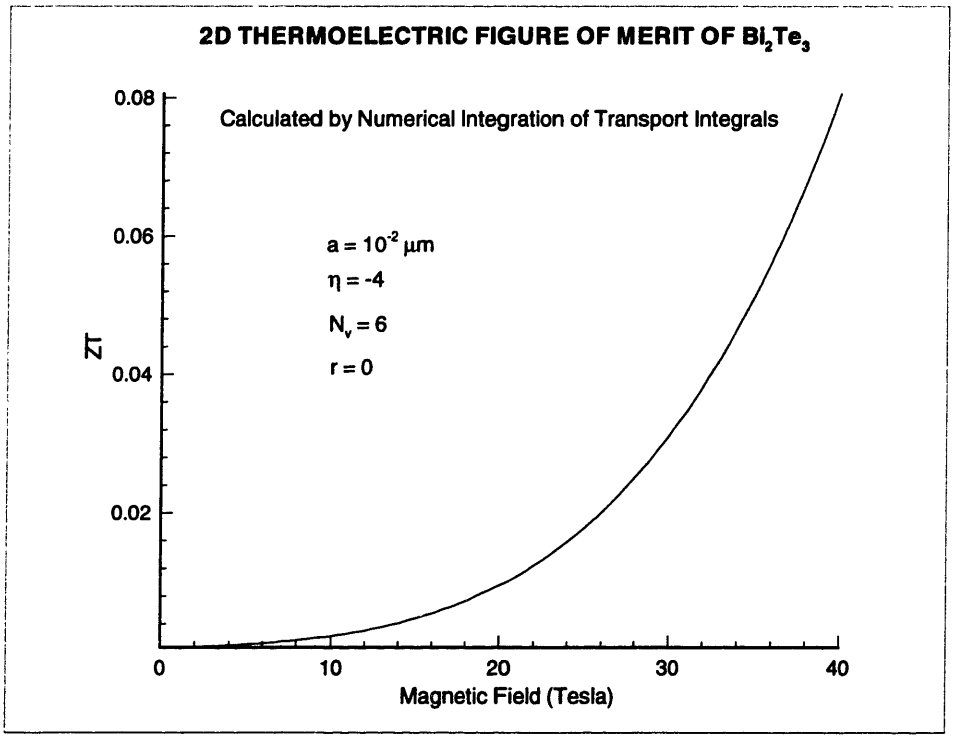


Figure 6-9: The dependence of the temperature normalized figure of merit on magnetic field is shown. $N_v = 6$ valleys with equal contributions are assumed. The scattering parameter $r = 0$ and the reduced Fermi energy $\eta = -4$. The thickness of the film is $100\mathring{A}$.

and $k_BT$ at room-temperature is 0.025 eV. This means for $Bi_2Te_3$ with $m_c^*/m_0 = 0.04$[3], the applied magnetic field has to be at least 10 Tesla.

Only the contribution of one-pocket is calculated. This pocket has the main axis of the ellipsoid parallel to the applied magnetic field. In two-dimensions and under conditions of Landau-level quantization, the valley degeneracy is split and contributions of each pocket require the calculation of individual cyclotron masses which take into account the orientation of each pocket relative to the magnetic field.

Despite the requirement that Landau-level mixing not occur, Equation 5.25 gives semi-quantitative results for diagonal conductivity $\sigma_{xx}$ when $\omega_c\tau \approx 1$. Below 5 Tesla, the approximation breaks down, yielding results which are sensitive to computational instability. These are not to be confused with the quantum effects due to Landau-level quantization (Figure 6-10). This instability is more dramatic in Figure 6-11 where the calculation is performed at a regime where the electron gas is non-degenerate. The reduced chemical potential at this low carrier density is $\eta = -4$.

At higher magnetic fields (Figure 6-12), the calculation is well-behaved. This curve is consistent with the expectation that the diagonal conductivity $\sigma_{xx}$ disappears at high magnetic fields. High scattering given by low mobility and low relaxation washes any peaks expected from quantization of **k**-space into Landau-levels.

A comparison between the effect of the functional forms of relaxation is shown on Figure 6-13. The energy and magnetic field dependent relaxation is given by Equation 5.22. The conductivity seems to converge at high values of magnetic field and diverges at lower values with the magnetic field dependent curve yielding a higher conductivity.

The result shown in Figure 6-14 is the calculation of $\sigma_{xx}$ using the Gaussian density of states (Equation ?? derived from the path-integral method. The calculation is well-behaved due to the absence of the non-physical cut-off of density states which occurs in the semi-elliptical form. A small change in curvature is apparent between 7 and 10 Tesla possibly due to the effect of quantized density of states.

[3]Using the diagonal effective mass tensor used by Hicks [6].

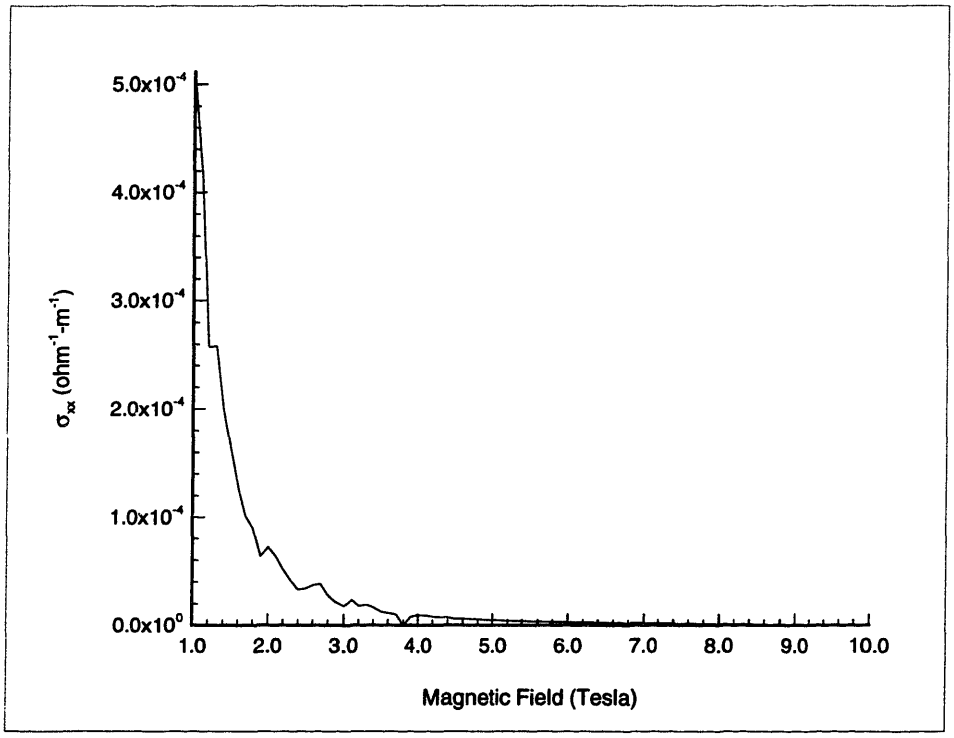


Figure 6-10: The magnetic field dependence of the diagonal conductivity $\sigma_{xx}$ of $Bi_2Te_3$ is simulated using a semi-elliptical density of states. The layer thickness $a = 300\mathring{A}$, the zero-field chemical potential $\eta = 1$, and $T = 300K$. The relaxation time is energy and magnetic field-dependent with a scattering parameter $r = 0$.

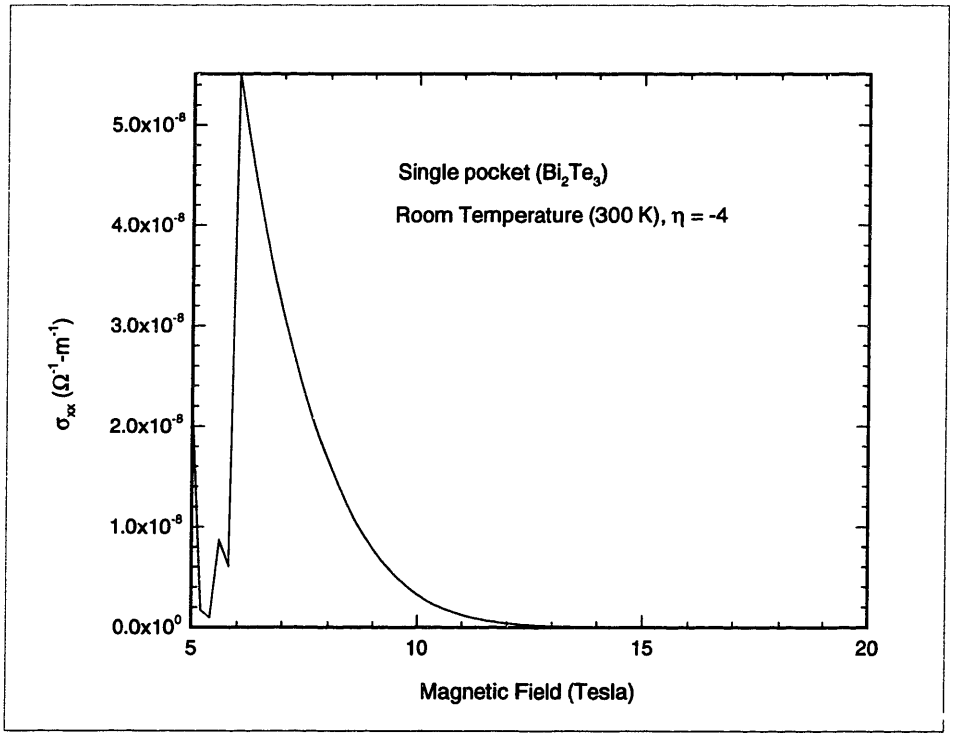


Figure 6-11: The magnetic field dependence of the diagonal conductivity $\sigma_{xx}$ of $Bi_2Te_3$ is simulated using a semi-elliptical density of states. The layer thickness $a = 300\mathring{A}$, the zero-field chemical potential $\eta = -4$, and $T = 300K$. The relaxation time is energy and magnetic field-dependent with a scattering parameter $r = 0$.

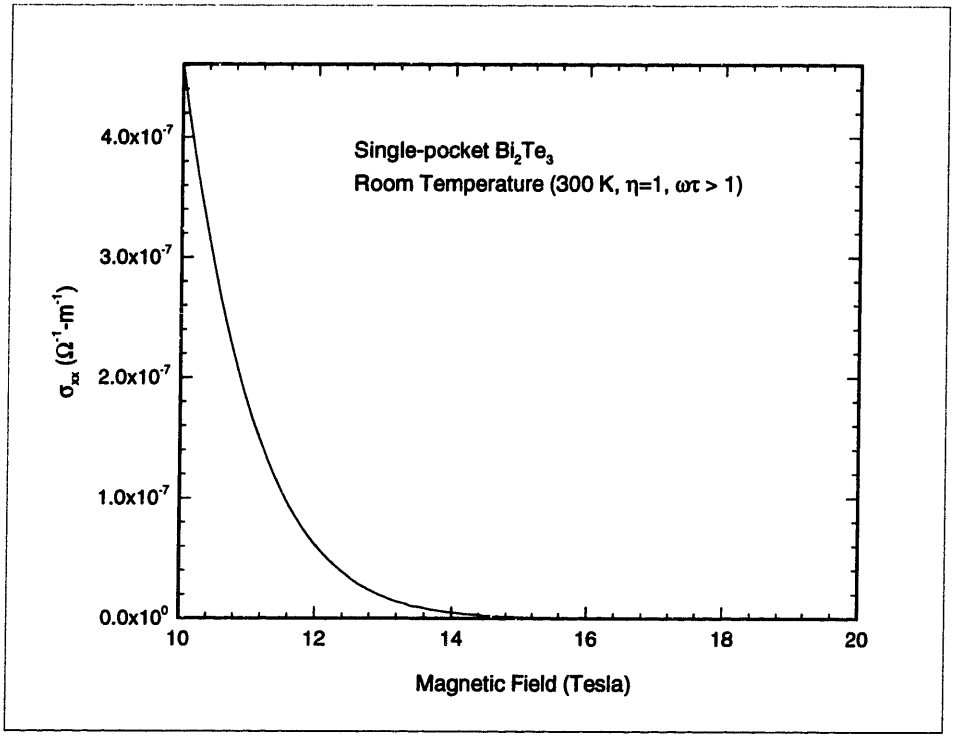


Figure 6-12: The magnetic field dependence of the diagonal conductivity $\sigma_{xx}$ of $Bi_2Te_3$ is simulated using a semi-elliptical density of states. The layer thickness $a = 300\mathring{A}$, the zero-field chemical potential $\eta = 1$, and $T = 300K$. The relaxation time is energy and magnetic field-dependent with a scattering parameter $r = 0$.

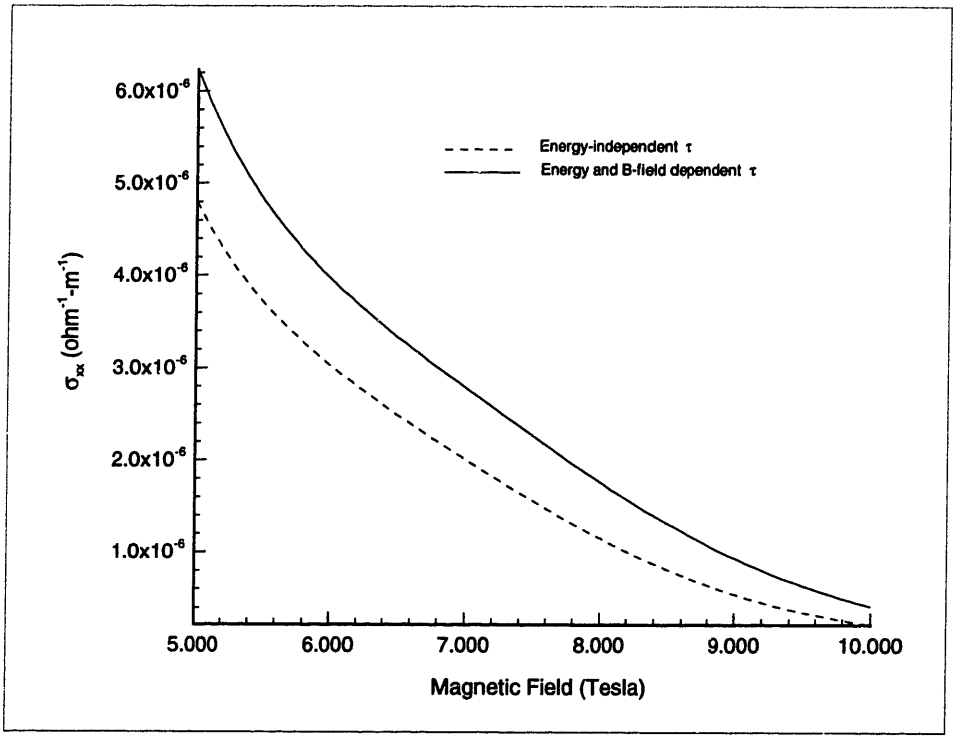


Figure 6-13: The magnetic field dependence of the diagonal conductivity $\sigma_{xx}$ is shown to affected by the functional form of the relaxation time $\tau$. The dashed curved is calculated given constant $\tau$ and the solid curve has $\tau = \tau_0(E + \hbar\omega_c/2)^{r-1/2}$ with $r = 0$.

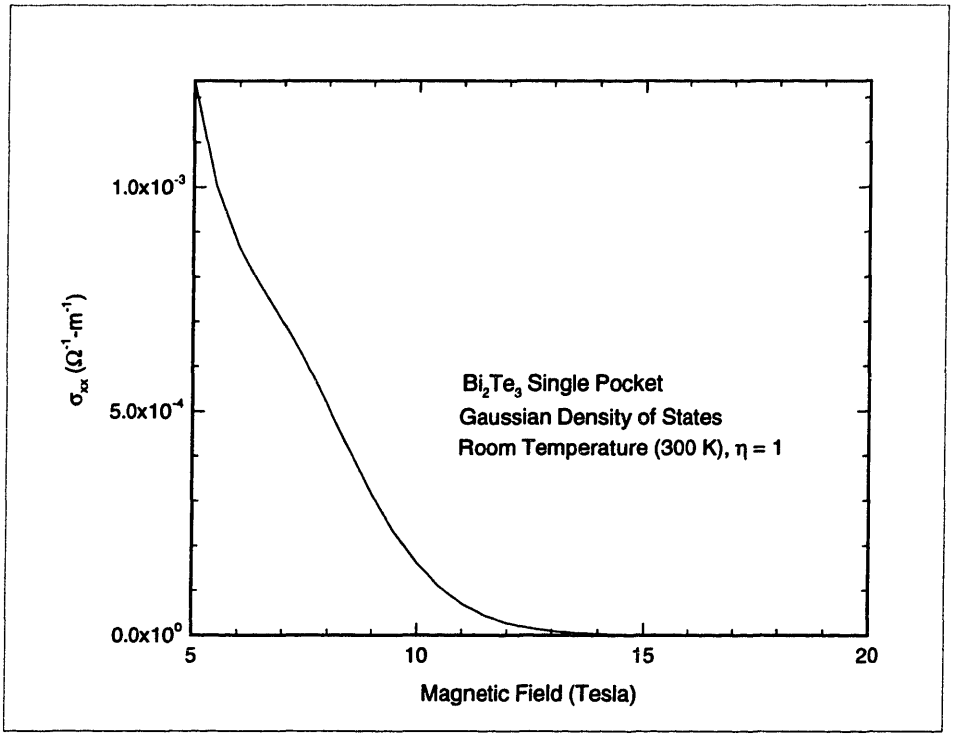


Figure 6-14: The magnetic field dependence of the diagonal conductivity $\sigma_{xx}$ of $Bi_2Te_3$ is simulated using a semi-elliptical density of states. The layer thickness $a = 300\mathring{A}$, the zero-field chemical potential $\eta = -1$, and $T = 300K$. The relaxation time is energy and magnetic field-dependent with a scattering parameter $r = 0$.

# Chapter 7

# Conclusion

A theoretical treatment on the effect of a magnetic field on the thermoelectric figure of merit ZT was presented. The treatment provided the basis for the numerical simulation of the behavior of ZT for arbitrary magnetic field, carrier concentration, and anisotropy. These simulations made extensive use of MATLAB and MAPLE.

The figure of merit was discussed in three dimensional case in the context of semiclassical calculations as a comparison to the detailed discourse on the two-dimensional case. ZT is a function of three transport coefficients: electrical conductivity, the Seebeck coefficient or thermopower, and the total thermal conductivity. The total thermal conductivity consists of contributions from electrons and phonons for energy transport. For any magnitude of applied magnetic field, the limiting factor in ZT is the phonon contribution to the thermal conductivity. The phonon thermal conductivity is an intrinsic property of the material. The other coefficients can be optimized relative to each other by varying the chemical potential by doping and by the application of a magnetic field.

The figure of merit was investigated at various ranges of magnetic field. The ranges of magnetic field can be categorized into three regions: the low-field or semiclassical case, the quantized or Landau-level case, and the high-field case. For each case, analytic expressions, or series approximations were calculated; the limitations of the expressions for each case were discussed,

The low-field case is treated in the context of the relaxation time approximation

of the semiclassical Boltzmann equation. Extensive investigation of valid and approriate approximations yielded analytic results which simplified numerical simulations. A low-field approximation with $\omega_c\tau \ll 1$ and a classical gas,or non-degenerate, approximation with $\eta \leq -4$ were useful in testing cases for comparison. Extensive series approximations and their regions of validity were presented. From the numerical simulations, it appears that higher gains in figure of merit are achievable for values of *eta* in the non-degenerate regime with the application of a magnetic field than for the degenerate or partially-degenerate cases. However, in practice, such low carrier densities is difficult to achieve in materials (mostly semiconductors or semimetals) with reasonable values for mobility. The reason for the limit on the carrier density seems to be the intrinsic carrier densities in those materials which are chosen for research as thermoelectrics.

The behavior of Landau-level quantization occurs when $\omega_c\tau > 1$. However, quantum effects such as the quantum Hall effect are not readily apparent at temperatures in which thermoelectric refrigeration finds its primary use. The reason that quantum effects become washed is due to large $k_BT$ compared to the Landau-level spacing. This results in large amounts of inter-Landau level scattering. It useful to find how it is possible for carriers to dump from carrier pockets with less than maximal contributions to ZT to pockets which can maximize ZT. Further work is necessary to determine the effectiveness of carrier dumping in enhancing ZT.

In addition to carrying out detailed calculations for carrier dumping, future work involves simulations of ZT at various regimes of magnetic field application at the optimized chemical potential $\eta$.

In conclusion, this thesis presents work which provides a basis for the estimation and calculation of various parameters with which to guide experimental research in the quest for the optimization of ZT.

# Bibliography


[1] Fowler Ando and Stern. Electronic properties of 2d systems. *Rev. Mod. Phys.*, 54(2), April 1982.

[2] S.M. Apenko and Y.E. Lozovik. Two-dimensional electron systems in magnetic field: high H as a classical limit. *J. Phys. C: Solid State Phys.*, 16:L591–L596, 1983.

[3] H.J. Goldsmid. *Thermoelectric Refrigeration.* The International Cryogenics Monograph Series. Plenum Press, New York, 1964.

[4] H.J. Goldsmid. *Electronic Refrigeration.* Pion, London, 1986.

[5] T.C. Harman and J.M. Honig. *Thermoelectric and Thermomagnetic Effects and Applications.* MacGraw-Hill, New York, 1967.

[6] L.D. Hicks and M.S. Dresselhaus. Effect of quantum-well structures on the thermoelectric figure of merit. *Physical Review B*, 47, May 1993.

[7] L.D. Hicks and M.S. Dresselhaus. Thermoelectric figure of merit of a one-dimensional conductor. *Physical Review B*, 47, June 1993.

[8] L.D. Hicks and M.S. Dresselhaus. Thermoelectric figure of merit of a one-dimensional conductor. *Physical Review B*, 47, June 1993.

[9] J.R. Hook and H.E. Hall. *Solid State Physics.* Manchester Physics Series. John Wiley and Sons, Chichester, England, second edition, 1991.

[10] R. Kubo, S. Miyake, and N. Hashitsume. Quantum theory of galvanomagnetic effect at extremely strong magnetic fields. In F. Seitz and D. Turnbull, editors, *Solid State Physics: Advances in Research and Applications*, volume 17, pages 269–364. Academic Press, New York, 1965.

[11] O. Madelung. *Introduction to Solid-State Theory.* Springer Series in Solid-State Sciences. Springer-Verlag, second edition, 1981.

[12] L. Smrcka and P. Streda. Transport coefficients in strong magnetic fields. *J. Phys. C: Solid State Phys.*, 10:2153–2161, 1977.

[13] J.M. Honig T.C. Harman and B.M. Tarmy. Galvano-thermomagnetic phenomena and the figure of merit in bismuth—i. transport properties of the intrinsic material. *Advanced Energy Conversion*, 5:1–19, 1965.

[14] J.M. Honig T.C. Harman and B.M. Tarmy. Galvano-thermomagnetic phenomena and the figure of merit in bismuth—ii: Survey of experimental data and calculation of device parameters. *Advanced Energy Conversion*, 5:181–203, 1965.

[15] J.M. Ziman. *Principles of the Theory of Solids.* Cambridge University Press, Cambridge, second edition, 1972.